

its electron correlation preferences. The $^5\Delta_g$ state is linear with three d^9s^1 Pt atoms involved in a three-center two-electron bond that is primarily d-like on the center Pt and s-like on the terminal Pt atoms. The metal-metal bonding is dominated by delocalized s-s interactions for the bent clusters, with the valence d electrons preferring to remain localized on each metal center. s-d hybridization does play a role in maximizing the overlap in what is primarily a 6s-6s bond (about 15-30% 5d) in all bent states, while we find s-p hybridization to be of negligible importance. The cohesive energy of Pt trimer (3A_1) with respect to three

separated ground-state Pt atoms (3D) is found to be at least 50.3 kcal/mol.

Acknowledgment. This work was supported by the Office of Naval Research (Grant No. N00014-89-J-1492) and partially by a grant from Aerojet Electrosystems. E.A.C. also acknowledges support from the National Science Foundation and the Camille and Henry Dreyfus Foundation through their Presidential Young Investigator and Distinguished New Faculty Award Programs.

Registry No. Pt₃, 110743-43-6.

Steric and Stereoelectronic Effects on Metal Ion Incorporation into Picket Fence Porphyrins in Homogeneous Solution: The Relationship of Molecular Conformation to Reactivity¹

David C. Barber, David S. Lawrence, and David G. Whitten*

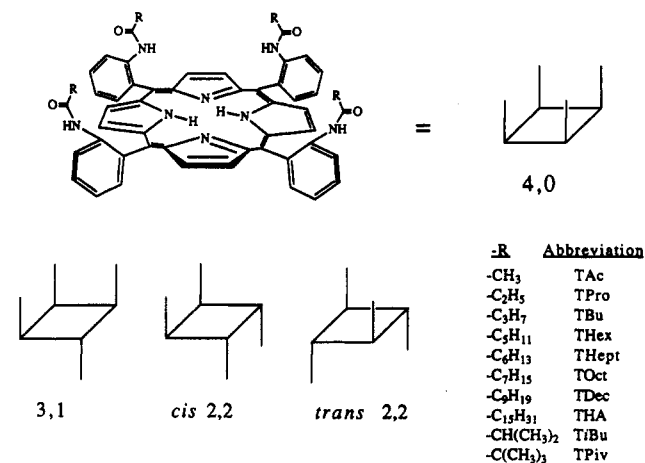
Department of Chemistry, University of Rochester, Rochester, New York 14627-0216
(Received: February 27, 1991; In Final Form: September 20, 1991)

Rate constants for the incorporation of Cu(II) and Zn(II) using the perchlorate salts were measured for the four atropisomers of C_2 and C_{16} derivatives of *meso*-tetrakis(*o*-alkylamidophenyl)porphyrin, the "picket fence" porphyrins (PFPs) in *N,N*-dimethylformamide (DMF). A 156-fold variation in rate constants is noted for Cu(II) incorporation into the 25 PFPs studied in DMF which are 56.5-8800 times less reactive than *meso*-tetraphenylporphyrin (TPP). For Cu(II) incorporation, the reactivity order is 4,0 > 3,1 > *cis* 2,2 > *trans* 2,2 in all cases. The span of metalation rate constants for individual isomers as a function of side chain length follows the opposite order, consistent with increasing steric exclusion of metal ion as the number of substituents (0-2) about the less hindered face of the porphyrin increases. A 2.2×10^5 -fold range of facial metalation rate constants calculated for TPP and the PFPs indicates that metalation of the 4,0 isomer occurs predominantly (>99%) from the unsubstituted face. Increased perpendicularity between the phenyl rings and the porphyrin core with increasing side chain bulk, attributed to (1) steric interactions between ortho substituents and the porphyrin core and (2) transannular side chain interactions, is postulated to result in enhanced core rigidity for the 4,0 isomer and consequent decreased metalation rates. This postulate is supported by ¹H NMR and UV-visible spectral data for the set of compounds studied, relative basicities, and molecular models. For the 4,0 isomer, whose metalation is controlled by such stereoelectronic factors, side chain branching more effectively inhibits metalation (range of $k_{Cu^{2+}} = 4.7 M^{-1} s^{-1}$) than linear side chain extension (range of $k_{Cu^{2+}} = 2.2 M^{-1} s^{-1}$). The results of this study are relevant to the spectroscopy, chemistry, and solution structure of tetraarylporphyrins.

Introduction

Extensive mechanistic studies of metal ion incorporation performed under various conditions with a wide variety of metal ions using natural and synthetic, water soluble and water insoluble free base porphyrins reveal that a variety of factors influence the rate of porphyrin metalation.²⁻⁹ Controlling factors of metalation include (1) solvent composition, (2) ligands attached to the metal ion center, (3) solvent or ligand exchange rates of the metal ion, (4) metal ion coordination geometry, (5) ionic strength, (6) total

CHART I: Picket Fence Porphyrin Structures and Atropisomer Representations



(1) Taken in part from the doctoral dissertation of David C. Barber, University of Rochester, 1989.

(2) Lavalley, D. K. *Coord. Chem. Rev.* 1985, 61, 55.

(3) Berezin, B. D. *Coordination Compounds of Porphyrins and Phthalocyanines*; John Wiley and Sons: New York, 1981.

(4) Longo, F. R.; Brown, E. M.; Rau, W. G.; Adler, A. D. In *The Porphyrins*; Dolphin, D., Ed.; Academic Press: New York, 1978; Vol. 5, pp 459-481.

(5) Hambricht, P. In *Porphyrins and Metalloporphyrins*; Smith, K. M., Ed.; Elsevier: Amsterdam, 1975; pp 233-278.

(6) Schneider, W. *Struct. Bonding (Berlin)* 1975, 23, 123.

(7) Hambricht, P. *Coord. Chem. Rev.* 1971, 6, 247.

(8) Falk, J. E., Lemberg, R., Morton, R. K., Eds. *Haematin Enzymes*; Pergamon: London, 1961.

(9) Falk, J. E. *Porphyrins and Metalloporphyrins*; Elsevier: Amsterdam, 1964; pp 35-40.

porphyrin charge, (7) the location of porphyrin charge with respect to the porphyrin center, (8) Hammett substituent constants of groups attached to the porphyrin, (9) deformability of the macrocyclic core, (10) accessibility of pyrrole nitrogen atoms to the

metal ion, and (11) N...H-N hydrogen bonding within the porphyrin core. Correlations between porphyrin basicities^{2,10-20} or reduction potentials^{21,22} and metalation rate constants have also been made for a wide variety of porphyrin structures, revealing inherent similarities among the three processes. A correlation of porphyrin basicities with enzymatic metalation rates (via soluble liver ferrochelatase) for nine natural dicarboxylic porphyrins demonstrates the relevance of metalation in homogeneous solution to biological porphyrin metalation^{23,24} and suggests a relationship between porphyrin core deformabilities and metalation rates. Thus a variety of factors, most notably porphyrin core deformation and geometric constraints of the metal ion complex in solution, account for porphyrin metalation being considerably slower than metal ion ligation by acyclic amines.²⁵

Relatively few studies have focused on the effect of structural variations within the porphyrin on metalation rates. For substituted *meso*-tetraphenylporphyrins (TPPs), the major structural features influencing metalation rates are ortho versus meta or para substitution,^{26,27} the location and extent of charges,^{11,16,28-30} Hammett substituent effects,³¹ and steric effects.^{27,32} While tetraphenyl- and tetraarylporphyrins have received much attention in metal ion incorporation studies, ortho-substituted TPPs^{11,16,18,26,28-36} and ortho-substituted TPPs, which produce four isolable atropisomers,^{27,29,32,33} have been less well studied. For Cu(II) incorporation into various tetra-ortho- and tetra-para-substituted TPPs, Hambright and Turay report that non-ortho-substituted TPPs and ortho-substituted TPPs containing small substituents are 50-200 times more reactive than the *meso*-tetrakis(*o*-pivalamidophenyl)porphyrins (the TPivs, see Chart I) in DMF²⁷ and that there are corresponding increases in porphyrin basicity and reactivity for para-substituted TPPs.^{26,37,38} Similarly,

Hatano and Anzai report that the TPiv atropisomers are less reactive than TPP toward Zn(II) in DMF.³² Overall, a systematic study of uncharged, ortho-substituted TPPs has been needed to definitively establish the consequences of chain length modification and structural variation between the four atropisomers on such properties as electronic spectra, ¹H NMR spectra, porphyrin rigidity, and porphyrin core basicity as well as the effects on rates of bimolecular reaction with metal ions.

We have previously reported discrimination in the reaction of Cu(II) with the short chain TAc atropisomers in 9:1 DMF/water.³⁹ Herein, we report a study of the effects of systematic variations of *o*-alkylamide substituent size and shape and atropisomer structure on relative metalation rates of the PFPs in an attempt to further elucidate the parameters controlling metalation of *meso*-tetraarylporphyrins. Notable findings are decreased facile metalation rate constants for metalation from the unhindered face of the 4,0 isomer⁴⁰ due to substitution on the other face of the molecule, steric control of reactivity as a function of metalating ion size, accelerated reactivities in 9:1 DMF/water for PFPs whose metalation is sterically controlled (the non-4,0 PFPs), and a decrease in core reactivities as a consequence of either *o*-amide substitution or transannular side chain interactions. The results of this study suggest that the phenyl ring/porphyrin core dihedral angle has a significant influence on the physical properties and reactivity of substituted TPPs and that more complex interactions may also be encountered in the PFPs.

Experimental Section

Materials and Methods. Solvents were analytical reagent grade or better. Soret maxima were obtained using an IBM 9430 UV-visible spectrophotometer, absorption maxima are ± 0.2 nm. Absorption spectra were recorded in 1-cm cells. CDCl₃ was chloroform-*d*, 99.8% (Cambridge Isotope Laboratories), and DMSO-*d*₆ was dimethyl sulfoxide-*d*₆ (Aldrich Chemical Co.).

Preparation of Picket Fence Porphyrin Derivatives. The PFPs were prepared by a modification of the method of Freitag and Whitten⁴¹ using individually isolated atropisomers of *meso*-tetrakis(*o*-aminophenyl)porphyrin (TAm).⁴² All rotary evaporations of PFP solutions were performed in the dark to prevent photoatropisomerization, and those of TAm solutions were performed in the dark on a room-temperature water bath to prevent thermal atropisomerization. Atropisomer identities have been established by X-ray crystallography for 4,0^{43,44} and trans 2,2⁴⁵ TAm derivatives while ¹H NMR spectroscopy distinguishes the 3,1 (three sets of side chain resonances) and cis 2,2 (two resolvable β -pyrrole resonances) isomers.⁴⁶ A statistical distribution of TAm isomers further supports the isomer assignments.^{43,47}

Metal Ion Incorporation Studies in Homogeneous Solution. All metal ion incorporation reactions were performed under pseudo-first-order conditions. Copper(II) incorporation studies were performed using copper(II) perchlorate hexahydrate (Aldrich Chemical Co.), *N,N*-dimethylformamide (certified ACS, Baker Analyzed Reagents) which was distilled from CaO and stored over molecular sieves, and water purified on a Milli-Q water purification system (Millipore Corp.). TPP was obtained from Aldrich Chemical Co. Reactions were initiated by syringe addition of the appropriate volume of Cu²⁺ in the desired solvent to a solution of the free base porphyrin in the reaction solvent. Reactions in

- (10) See ref 9, p 35.
 (11) Adeyemo, A.; Shamim, A.; Hambright, P.; Williams, R. F. X. *Indian J. Chem.* **1982**, *21A*, 763.
 (12) Shah, B.; Shears, B.; Hambright, P. *Inorg. Chem.* **1971**, *10*, 1828.
 (13) Meot-Ner, M.; Adler, A. D. *J. Chem. Soc.* **1972**, *94*, 4763.
 (14) Berezin, B. D.; Koifman, O. I. *Russ. J. Phys. Chem. (Engl. Transl.)* **1972**, *46*, 24.
 (15) Berezin, B. D.; Koifman, O. I. *Russ. J. Phys. Chem. (Engl. Transl.)* **1971**, *45*, 820.
 (16) Reid, J. B.; Hambright, P. *Inorg. Chem.* **1977**, *16*, 968.
 (17) Turay, J.; Hambright, P. *J. Inorg. Nucl. Chem.* **1979**, *41*, 1385.
 (18) Turay, J.; Hambright, P. *Inorg. Chim. Acta* **1979**, *35*, L319.
 (19) Shears, B.; Shah, B.; Hambright, P. *J. Am. Chem. Soc.* **1971**, *93*, 776.
 (20) Hambright, P. *Inorg. Chem.* **1977**, *16*, 2987.
 (21) Williams, R. F. X.; Hambright, P. *Bioinorg. Chem.* **1978**, *9*, 537.
 (22) Worthington, P.; Hambright, P.; Williams, R. F. X.; Reid, J.; Burnham, C.; Shamim, A.; Turay, J.; Bell, D. W.; Dirkland, R.; Little, R. G.; Datta-Gupta, N.; Eisner, U. *J. Inorg. Biochem.* **1980**, *12*, 281.
 (23) See ref 9, pp 39-40.
 (24) Porra, R. J.; Jones, O. T. G. *Biochem. J.* **1963**, *87*, 186.
 (25) Schneider, W. *Struct. Bonding (Berlin)* **1975**, *23*, 139.
 (26) Longo, F. R.; Brown, E. M.; Quimby, D. J.; Adler, A. D.; Meot-Ner, M. *Ann. N. Y. Acad. Sci.* **1973**, *206*, 420.
 (27) Turay, J.; Hambright, P. *Inorg. Chim. Acta* **1981**, *53*, L147.
 (28) Choi, E. I.; Fleischer, E. B. *Inorg. Chem.* **1963**, *2*, 94.
 (29) Buckingham, D. A.; Clark, C. R.; Webley, W. S. *J. Chem. Soc., Chem. Commun.* **1981**, 192.
 (30) Kassner, R. J.; Wang, J. H. *J. Am. Chem. Soc.* **1966**, *88*, 5170.
 (31) James, J.; Hambright, P. *Inorg. Chem.* **1973**, *12*, 474.
 (32) Anzai, K.; Hatano, K. *Chem. Pharm. Bull.* **1984**, *32*, 2067.
 (33) Valiotti, A.; Adeyemo, A.; Williams, R. F. X.; Ricks, L.; North, J.; Hambright, P. *J. Inorg. Nucl. Chem.* **1981**, *43*, 2653.
 (34) Thompson, A. N.; Krishnamurthy, M. *J. Inorg. Nucl. Chem.* **1979**, *41*, 1251.
 (35) Nwaeme, J.; Hambright, P. *Inorg. Chem.* **1984**, *23*, 1990.
 (36) Shamim, A.; Hambright, P. *Inorg. Chem.* **1983**, *22*, 694.
 (37) Jones, S.; Po, H. N. *Inorg. Chim. Acta* **1980**, *42*, 95.
 (38) Turay, J.; Hambright, P. *Inorg. Chem.* **1980**, *19*, 562.

(39) Barber, D. C.; Whitten, D. G. *J. Am. Chem. Soc.* **1987**, *109*, 6842.

(40) The atropisomer notations 4,0, 3,1, cis 2,2, and trans 2,2 have also been referred to as $\alpha,\alpha,\alpha,\alpha$, $\alpha,\alpha,\alpha,\beta$, $\alpha,\alpha,\beta,\beta$, and $\alpha,\beta,\alpha,\beta$; see ref 43.

(41) Freitag, R. A.; Whitten, D. G. *J. Phys. Chem.* **1983**, *87*, 3918.

(42) Barber, D. C.; Freitag-Beeston, R. A.; Whitten, D. G. *J. Phys. Chem.* **1991**, *95*, 4074.

(43) Collman, J. P.; Gagne, R. R.; Reed, C. A.; Halbert, T. R.; Lang, G.; Robinson, W. T. *J. Am. Chem. Soc.* **1975**, *97*, 1427.

(44) Collman, J. P.; Gagne, R. R.; Reed, C. A.; Robinson, W. T.; Rodley, G. A. *Proc. Natl. Acad. Sci. USA* **1974**, *71*, 1326.

(45) Scheidt, T. Q.; Eigenbrot, C. W.; Ogiso, M.; Hatano, K. *Bull. Chem. Soc. Jpn.* **1987**, *60*, 3529.

(46) Barber, D. C.; Whitten, D. G. Unpublished results.

(47) Hatano, K.; Kawasaki, K.; Munakata, S.; Iitaka, Y. *Bull. Chem. Soc. Jpn.* **1987**, *60*, 1985.

TABLE I: Cu(II) Incorporation Rate Constants for the Picket Fence Porphyrins in DMF

porphyrin	4,0 isomer			3,1 isomer			cis 2,2 isomer			trans 2,2 isomer		
	k^a	$(k_{rel})^b$	av % decrease ^c	k^a	$(k_{rel})^b$	av % decrease	k^a	$(k_{rel})^b$	av % decrease	k^a	$(k_{rel})^b$	av % decrease
TPP	40020	(8800)										
TAc	709	(156)	32.7	70.1	(15.4)		46.6	(10.2)		24.9	(5.48)	
TPro	515	(113)	27.3	59.2	(13.0)	15.6	38.1	(8.36)	18.3	21.4	(4.71)	14.1
TBu	404	(88.8)	21.5									
THex	382	(83.8)	2.8	29.4	(6.47)	16.8	18.5	(4.06)	17.1	5.92	(1.30)	24.1
THept	367	(80.7)	3.8									
TOct	356	(78.1)	3.2									
TDec	334	(73.5)	3.0									
THA	323	(71.0)	0.5	19.7	(4.32)	3.3	10.9	(2.40)	4.1	4.55	(1.00)	2.3
TiBu	319	(70.1)	38.1 ^d									
TPiv	150	(32.9)	53.1	63.0	(13.8)		33.0	(7.24)		26.2	(5.76)	
$k(\text{TAc})/k(\text{THA})$		2.19			3.56			4.25			5.48	

^a $k_{obs}/[\text{Cu(II)}]$; values expressed in $\text{M}^{-1} \text{s}^{-1} \times 10^6$. ^b Relative rate constants; values expressed relative to $k_{trans\ 2,2\ \text{THA}} = 1.0$. ^c The average percentage decrease in metalation rate constant relative to the previous table entry for the same isomer divided by the number of added side chain carbon or nitrogen atoms in a linear or branched (for TiBu and TPiv) fashion. ^d Value calculated from TPro as the previous table entry based on side chain branching.

DMF and 9:1 DMF/water, in which porphyrin and Cu^{2+} are cosoluble, were performed at $[\text{Cu}^{2+}] = 0.15\ \text{M}$. Porphyrin concentrations were 25–30 μM , as measured by UV-visible absorption; under these conditions, the porphyrins were not aggregated as evidenced by superposable normalized absorption spectra in the Soret region for concentrated and dilute solutions measured in 1-mm and 1-cm cells, respectively. A first-order dependence on metal ion concentration was observed for TPP from 3.75 to 150 mM $\text{Cu}(\text{ClO}_4)_2$ in DMF, comparable to the results noted by Tanaka in very dry DMF solution (see ref 74); the reaction between CuSO_4 and TPP exhibited rate saturation with increasing $[\text{Cu}^{2+}]$ over the same range of Cu(II) concentration in DMF. Zn(II) incorporation reactions were performed at a zinc(II) perchlorate (Pfaltz & Bauer) concentration of 0.19 M and 44–96 μM porphyrin. All metalation reactions were performed in acid-washed glass cuvettes (hot aqua regia, overnight) sealed with a septum cap. UV-visible spectra were recorded between 480 and 700 nm using a Hewlett-Packard 8451A diode array spectrophotometer and stored to disk. Metalation rates were measured at least in duplicate at ambient temperature (20–22 °C). For sets of samples measured at different times or with different batches of solvent, a control was run with TPP.

Calculation of Metalation Rate Constants. Metalation rate constants were calculated using a linear least-squares program on an HP 8451A diode array spectrophotometer to determine the slope of $\ln \Delta A$ vs time data obtained during reaction. Pseudo-first-order plots were linear for Cu(II) incorporation throughout the reaction while those for Zn(II) incorporation were linear after the first 10–20% reaction, as previously reported with the TPiv isomers.³² Metalation reactions were first order in $[\text{H}_2\text{P}]$ under pseudo-first-order conditions where metal ion concentration is in large (>1000-fold) excess. Rates measured in the Soret and visible regions (i.e., at ~420, 516, and 550 nm) were in good agreement, generally giving correlation coefficients ≥ 0.998 . The agreement between rate constants taken as the average value obtained at two or three analysis wavelengths was generally $\pm 5\%$ or better, unless otherwise indicated.

¹H NMR Spectral Measurements. NMR spectra were recorded on a General Electric 300-MHz QE-300 NMR in CDCl_3 . Resonance frequencies were calibrated using a solvent deuterium lock.

Apparent Basicities in 9:1 DMF/Water. Aliquots (3 mL) of porphyrin in 9:1 DMF/water were titrated in a cuvette by addition of 1–10 μL aliquots of aqueous HCl (1, 10, 100, 1000, and 5000 mM HCl) prepared by dilution of stock 1.0 M aqueous HCl (Fisher 1.0 N HCl, Fisher Scientific) or concentrated hydrochloric acid (36.5–38.0% Baker Analyzed Reagent). Spectra were recorded upon each addition of acid, and equivalence points were determined by spectral measurement of the relative amounts of free base porphyrin (H_2P , $\lambda_{max} = \sim 420\ \text{nm}$) and diacid (H_4P^{2+} , $\lambda_{max} = \sim 427\ \text{nm}$) forms present at each acid concentration.

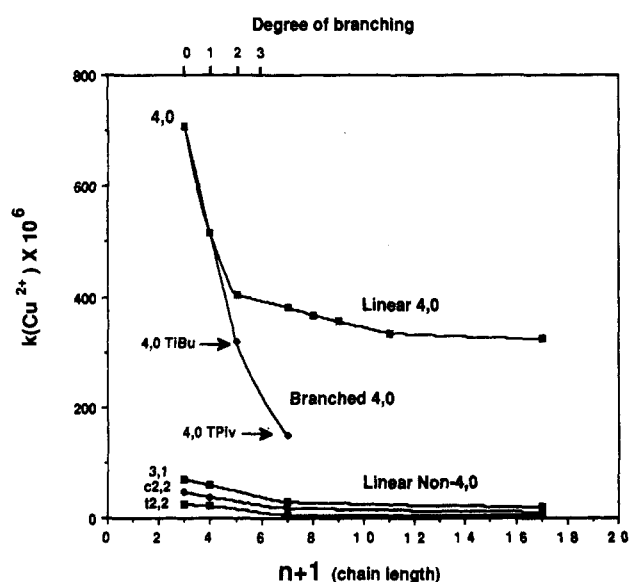


Figure 1. Effect of "picket" length and branching on Cu(II) incorporation rate constants: (□) linear 4,0 PFPs; (◆) branched 4,0 PFPs; (□) 3,1 PFPs; (○) cis 2,2 PFPs; (■) trans 2,2 PFPs.

Spectra of the H_2P and H_4P^{2+} forms were obtained from spectra taken prior to addition of acid and after the addition of 1–2 drops of concentrated hydrochloric acid (36.5–38.0%, Baker Analyzed Reagent) at the end of each titration to assure complete conversion to H_4P^{2+} , respectively. The apparent $\text{p}K_3K_4$ values were calculated as twice the expected pH of an aqueous solution to which the amount of acid required to reach the equivalence point (i.e., $[\text{H}_2\text{P}] = [\text{H}_4\text{P}^{2+}]$) had been added.

Results and Discussion

Cu(II) Incorporation in DMF. Rate constants for Cu(II) incorporation into the PFPs under pseudo-first-order conditions in *N,N*-dimethylformamide solution are displayed in Table I. Metalation rate constants for the 25 PFPs span a range of 156 in DMF; the overall range including TPP is 8800. Regular reactivity trends are observed for a wide variety of structures as a function of atropisomer, side chain length, and side chain branching (see Figure 1). The order of relative Cu(II) incorporation rate constants for the four PFP atropisomers (i.e., 4,0 > 3,1 > cis 2,2 > trans 2,2) regardless of side chain identity is consistent with more efficient metalation from the less hindered porphyrin face. Thus, the 4,0 isomer, with a totally unhindered face for metalation, is the most reactive while the 3,1 isomer, with one singly hindered face, is the second most reactive. The cis and trans 2,2 isomers experience equal steric shielding from both sides, resulting in a greater net reduction in metalation rate constant.

TABLE II: Facial Metalation Rate Constants for Cu(II) Incorporation in DMF^a

H ₂ P	<i>n</i>	$k(0,n)_{\text{est}}^b$	$k(1,n)_{\text{est}}^c$	$k(2,n)_{\text{adj}}^{d,e}$	$k(2,n)_{\text{opp}}^{e,f}$	$k(3,n)_{\text{est}}^g$	$k(4,n)_{\text{est}}^h$
DMF							
TPP	0	20010 ^{e,i}					
TAc	2	707.4 ± 0.2	65.06 ± 7.7	23.30	12.45	5.04	1.09
TPro	3	513.9 ± 0.2	54.99 ± 7.7	19.05	10.70	4.21	0.93
THex	6	381.5 ± 0.2	28.36 ± 3.7	9.25	2.96	1.04	0.12
THA	16	323.3 ± 0.03	18.99 ± 3.8	5.45	2.28	0.713	0.093
TPiv	tBu	148.5 ± 0.77	59.56 ± 5.8	16.5	13.1	3.44	1.14
9:1 DMF/Water							
TAc	2	713.9 ± 1.0	119.2 ± 15.8	50.0	37.55	18.78	7.06

^a Calculated using values in Tables I, II, and VII; expressed in M⁻¹ s⁻¹ × 10⁶. ^b $k(0,n)_{\text{est}} = k_{4,0} - k(4,n)_{\text{est}}$. ^c $k(1,n)_{\text{est}} = k_{3,1} - k(3,n)_{\text{est}}$. ^d $k(2,n)_{\text{adj}} = k_{\text{cis } 2,2}/2$. ^e Actual value. ^f $k(2,n)_{\text{opp}} = k_{\text{trans } 2,2}/2$. ^g $k(3,n)_{\text{est}} = k(2,n)_{\text{opp}}/R_{1 \rightarrow 2\text{opp}}$, where $R_{1 \rightarrow 2\text{opp}} = k(1,n)_{\text{min}}/k(2,n)_{\text{opp}}$. ^h $k(4,n)_{\text{est}} = k(2,n)_{\text{opp}}/[R_{1 \rightarrow 2\text{adj}}R_{1 \rightarrow 2\text{opp}}]$, where $R_{1 \rightarrow 2\text{adj}} = k(1,n)_{\text{min}}/k(2,n)_{\text{adj}}$. ⁱ $k(0,0)$.

The regular decrease in metalation rate constant upon side chain extension for the 3,1, cis 2,2, and trans 2,2 isomers (see Table I) is commensurate with direct steric inhibition of reactivity due to the net bulk of the side chain "pickets". The order of the ranges of reactivity for an individual isomer as a function of side chain length (i.e., $k_{\text{TAc}}/k_{\text{THA}}$ values follow the order trans 2,2 (5.48) > cis 2,2 (4.25) > 3,1 (3.56) > 4,0 (2.19); see Table I) further indicates that steric effects are more pronounced with increasing number of substituents about the less hindered face of the porphyrin (i.e., 0–2). A general increase in the ranges of metalation rate constants for the four atropisomers with increasing chain length (i.e., for TAc, TPro, THex, and THA, $k_{4,0}/k_{\text{trans } 2,2} = 24.5, 24.1, 64.5,$ and $71.1,$ respectively) evidences the dominant role of direct steric effects on Cu(II) incorporation into the PFPs. Furthermore, molecular models clearly indicate that the side chains should sterically hinder approach of a solvated metal ion to the porphyrin core.

Facial Metalation Rate Constants. The observed Cu(II) incorporation rate constants can be divided into two "facial" metalation rate constants, one for metalation from each porphyrin face; these can be represented in the form

$$k(a,n)_s$$

where k represents a rate constant for metalation via a face bearing a alkylamide chains of n linear carbon atoms in the side chain and s is the side chain arrangement code when $a = 2$, depicting the arrangement of side chains in either the cis 2,2 or trans 2,2 isomers (i.e., adj = adjacent chains and opp = opposite chains), as shown in Figure 2. For each of the four isomers, the observed metalation rate constants can then be expressed as the sum of their facial metalation rate constants. Thus, $k_{\text{TPP}} = 2k(0,0)$, and in general, $k_{4,0} = k(4,n) + k(0,n)$, $k_{3,1} = k(3,n) + k(1,n)$, $k_{\text{cis } 2,2} = 2k(2,n)_{\text{adj}}$, and $k_{\text{trans } 2,2} = 2k(2,n)_{\text{opp}}$.

From the cis 2,2, trans 2,2, and TPP data, we can directly obtain $k(2,n)_{\text{adj}}$, $k(2,n)_{\text{opp}}$, and $k(0,0)$ (see Table II). Facial metalation rate constants can be approximated for the 4,0 and 3,1 isomers for which the observed metalation rate constant is the sum of two different facial metalation rate constants. Although these values cannot be determined precisely, estimates of $k(0,n)$, $k(1,n)$, $k(3,n)$, and $k(4,n)$ for all chain lengths studied can be obtained as follows. Assuming that facial metalation rate constants are largely controlled by direct steric factors based on the number of side chain appendages per face (i.e., 0, 1, 2, 3, or 4), as evidenced by the fact that the facial metalation rate constant for the trans 2,2 isomer, $k(2,n)_{\text{opp}}$, is 6–140 times lower than the metalation rate constants for either of the corresponding 4,0 or 3,1 isomers, the 4,0 and 3,1 PFPs must metalate predominantly from their less hindered face. Therefore, $k(2,n)_{\text{opp}}$ values can be taken as an upper estimate of $k(4,n)$ and $k(3,n)$. Lower estimates for $k(0,n)$ and $k(1,n)$ can be calculated as $k(0,n)_{\text{min}} = k_{4,0} - k(4,n)_{\text{max}}$ and $k(1,n)_{\text{min}} = k_{3,1} - k(3,n)_{\text{max}}$. Considering that the degree of reduction in facial metalation rate constants expected for additional mono- or disubstitution on a face of the trans 2,2 isomer is multiplicative in the 3,1 and 4,0 isomers, the ratios of metalation rate constants, i.e. $R_{1 \rightarrow 2\text{adj}}$ and $R_{1 \rightarrow 2\text{opp}}$, can be used to calculate refined estimates of $k(3,n)$ and $k(4,n)$ as described in Table II;

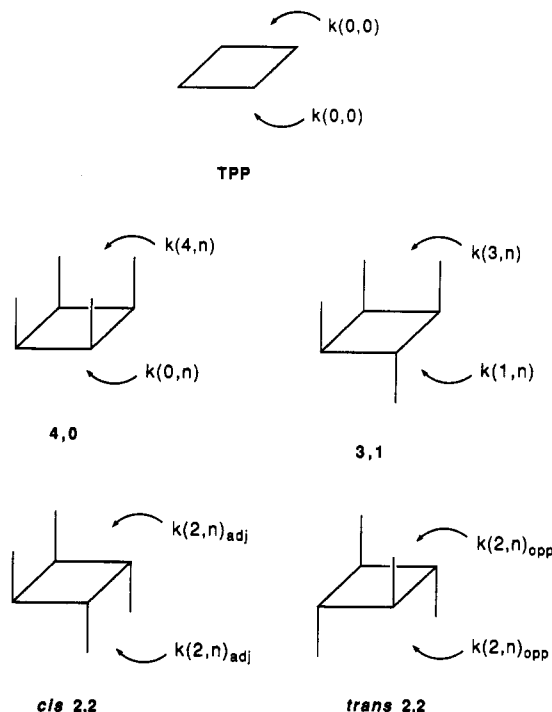


Figure 2. Facial metalation rate constants for TPP and the PFP atropisomers.

$R_{1 \rightarrow 2\text{adj}}$ represents the factor of rate reduction upon addition of a facial substituent adjacent to a preexisting substituent, and $R_{1 \rightarrow 2\text{opp}}$ represents the rate reduction factor upon addition of a substituent opposite to a preexisting facial substituent.

The calculated facial metalation rate constants evidence strong direct and indirect steric effects on Cu(II) incorporation. A 2.2×10^5 -fold range of facial metalation rate constants are calculated between an unhindered face of TPP and the most hindered PFP face in DMF. For 4,0 THA, the greatest disparities in facial rate constants are noted, where the estimated metalation rate from the unsubstituted face is ~3500 times greater than that from the tetrasubstituted face (i.e., $k(0,16)_{\text{est}}/k(4,16)_{\text{est}} = 3500$). In DMF, $k(0,n)_{\text{est}}$ values are 10–20-fold higher than $k(1,n)_{\text{est}}$ values while the addition of an adjacent or opposite side chain to a singly hindered face results in approximately 3-fold and 5–9-fold decreases in facial metalation rate constant. From the data in Table II, we conclude that metalation from the hindered face of the 4,0 isomer is negligible; metalation from the unhindered face of the 4,0 isomer accounts for 99.2–99.97% of the observed Cu(II) incorporation rate constant in DMF. Similarly, 99.0% of the Cu(II) insertions into 4,0 TAc occur via the unsubstituted face in 9:1 DMF/water. Likewise, metalation from the less hindered face of the 3,1 isomer accounts for ~92–96% of $k_{3,1}$ isomer in DMF and ~84% of $k_{3,1}$ TAc in 9:1 DMF/water. Thus, $k(0,n)$ values are almost exactly equal to $k_{4,0}$ isomer and $k(3,n)$ values are approximated by $k_{3,1}$ isomer. Curiously, the facial metalation rate constant from the unsubstituted face of 4,0 PFPs decreases with

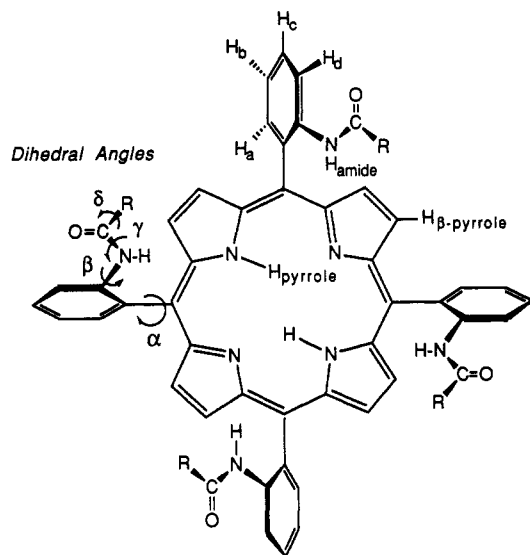


Figure 3. ^1H NMR assignments and dihedral angles in the PFPs.

increasing steric bulk on the opposite face which is attributed to indirect conformational effects as discussed below.

Stereoelectronic Effects on Cu(II) Incorporation into the PFPs. Direct steric exclusion of the metal ion from the porphyrin core can only partially account for the observed Cu(II) incorporation trends as is evident by comparing the reactivity of TPP to that of the 4,0 PFPs (see Table I). Addition of an acetamide group to the ortho position of TPP causes a significant reduction in the metalation rate constant (i.e., $k_{\text{TPP}}/k_{4,0\text{TAc}} = 56.5$) whereas a reactivity decrease of, at most, a factor of 2 could be attributed to the complete steric exclusion of the metal ion from one face of 4,0 TAc. The reactivity of straight chain 4,0 PFPs decreases by a factor of ~ 2 as the amide chain length increases from 2 to 16 carbons (i.e., $k_{4,0\text{TAc}}/k_{4,0\text{THA}} = 2.2$), and a greater decrease is observed with *o*-alkylamide substituent branching at the third atom of the side chain (i.e., $k_{4,0\text{TAc}}/k_{4,0\text{TPiv}} = 4.7$). The greatest difference in facial metalation rate constants for an unsubstituted face, $k(0,0)/k(0,t\text{Bu})$, is a factor of 135. Since metalation of the 4,0 isomer occurs almost exclusively from the unhindered face, the decreases in $k_{\text{Cu}^{2+}}$ with increasing substituent bulk suggests that the inherent reactivity of the porphyrin core differs as a function of side chain length in the 4,0 isomer; it is reasonable to assume that a similar effect may also be operative for the other atropisomers, although less readily separated from direct steric effects.

We attributed reduced reactivities of the 4,0 PFPs to enhanced core rigidity due to changes in the phenyl ring conformation resulting from steric interactions between (1) the ortho substituent and atoms of the pyrrole rings (referred to as the "ortho effect") and (2) steric interactions between cofacial side chains ("transannular" steric effects, see below) both of which disrupt coplanarity between the phenyl rings and the porphyrin core. According to molecular models, transannular steric contact is only possible for PFPs with C_3 or longer side chains. The aromatic rings of *meso*-tetraarylporphyrins lie partially perpendicular to the plane of the porphyrin macrocycle, especially in the crystalline state, due to steric interactions between the aryl groups and β -pyrrole hydrogen atoms of the porphyrin ring.⁴⁸⁻⁵⁰ Although crystal structures report 60 and 81.5° dihedral angles, α , between the porphyrin core and phenyl rings of TPP in the solid state,^{48,49} a 40° dihedral angle has been estimated for TPP in solution,⁵¹ yielding a large latitude of α values (i.e., $40^\circ \leq \alpha \leq 90^\circ$, see Figure 3) as a function of ortho-substituent bulk for substituted TPPs. Ortho substitution increases the phenyl-to-core dihedral angle,

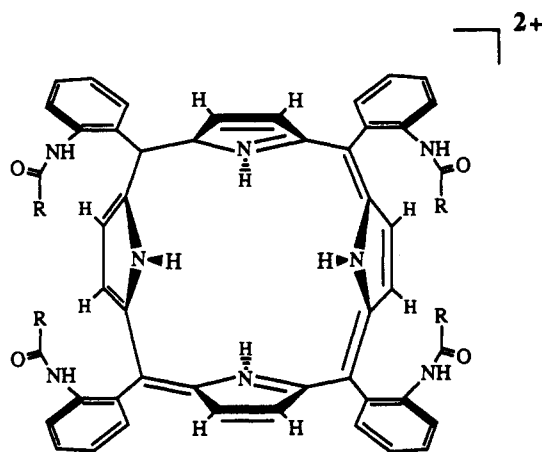
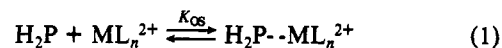


Figure 4. Depiction of a 4,0 PFP diacid.

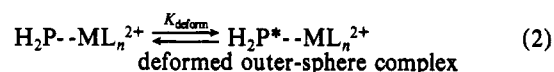
α , and, more importantly, should restrict α upon core deformation as required for metalation, as in the tetraarylporphyrin diacids.^{41,52,53} Resonance stabilization of a deformed core occurs due to enhanced coplanarity between phenyl rings and the porphyrin core in the TPP diacid, $\text{H}_4\text{TPP}^{2+}$, and by delocalization of cationic charge resulting from core diprotonation or, in the case of metalloporphyrin formation, due to metal-to-core nitrogen bonding, since loss of the two core protons is not rate determining.^{18,29,54-56} This situation (i.e., formation of a doubly bonded metal-to-porphyrin intermediate during metalation, intermediate B, see Scheme I) is analogous to protonation of the two core

SCHEME I: Mechanism for Porphyrin Metalation

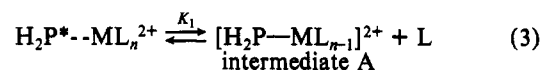
step 1: outer-sphere complexation



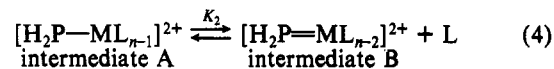
step 2: porphyrin deformation



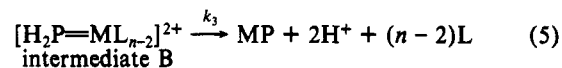
step 3: first bond formation



step 4: second bond formation



step 5: rapid final incorporation



pyrrole nitrogen atoms of TPP which causes the pyrrole rings of the TPP diacid to tilt alternatively above and below the plane of the porphyrin core by an angle of 33°, as noted by X-ray crystallography.^{52,57} Reduced steric interaction between the *o*-phenyl and β -pyrrole hydrogens permit the phenyl rings to attain a more coplanar arrangement with respect to the mean plane of the porphyrin diacid as indicated in Figure 4 and reduces atropisomerization barriers for the PFPs by 2-3 kcal/mol.⁴¹ From X-ray crystallography, a 21° phenyl ring-macrocycle dihedral angle, α , is reported for $\text{H}_4\text{TPP}^{2+}$.^{52,57} Accordingly, absorption

(48) Hoard, J. L.; Hamor, M. J.; Hamor, T. A. *J. Am. Chem. Soc.* **1963**, *85*, 2334.

(49) Silvers, S.; Tulinsky, A. *J. Am. Chem. Soc.* **1964**, *86*, 927.

(50) Fleischer, E. B. *J. Am. Chem. Soc.* **1963**, *85*, 1353.

(51) Wolberg, A. *J. Mol. Struct.* **1974**, *21*, 61.

(52) Fleischer, E. B.; Stone, A. J. *Chem. Soc., Chem. Commun.* **1967**, 332.

(53) Gunter, M. J.; Mander, L. N. *J. Org. Chem.* **1981**, *46*, 4792.

(54) Baum, S. J.; Plane, R. A. *J. Am. Chem. Soc.* **1966**, *88*, 910.

(55) Weaver, J.; Hambricht, P. *Inorg. Chem.* **1969**, *8*, 167.

(56) Shamim, A.; Hambricht, P.; Williams, R. F. X. *Inorg. Nucl. Chem. Lett.* **1979**, *15*, 243.

(57) Fleischer, E. B.; Stone, A. L. *J. Am. Chem. Soc.* **1968**, *90*, 2735.

spectral shifts observed upon core diprotonation of TPP and various PFPs attribute the substantial total visible band red shift for TPP (+30 nm vs -10 to +22 nm for the PFP diacids)⁴¹ to greater resonance interaction between the phenyl ring and porphyrin π systems. Hence, core deformabilities are directly related to the degree of resonance interaction possible between *meso*-phenyl rings and the porphyrin core as limited by steric interactions between ortho substituents and the pyrrole rings, and thus, Cu(II) incorporation into 4,0 TAc occurs 57 times slower than into TPP.

The effect of *o*-phenyl substitution on TPP, analogous to the situation in 2,6-disubstituted biphenyls⁵⁸ and as evidenced by high atropisomerization barriers for ortho-substituted tetraphenylporphyrins ($\Delta G^*_{\text{atrop}} = 15.6\text{--}17.9, 29.1, 29.1, \text{ and } 30.5$ kcal/mol for non-ortho-substituted metallo-TPPs,^{59,60} 4,0 TPro, 4,0 THA, and 4,0 TPiv,⁴¹ respectively, hence the predicted order of phenyl-to-core dihedral angles, α), clearly reduces core reactivities by an "ortho" effect; core reactivities also differ as a function of atropisomer structure and side chain bulk in such a way that they suggest a secondary effect arising from transannular steric interactions. While atropisomerization barriers do not differ significantly for 4,0 TPro or 4,0 THA as compared to that of 4,0 TPiv, indicating similar degrees of steric interaction between *o*-phenyl substituents and β -pyrrole hydrogen atoms, core reactivities toward Cu(II) incorporation differ by a factor of 4.7, a difference attributed almost entirely (>99%) to differences in the metalation rate constant from their unhindered face (i.e., $k(0,\pi)$). Furthermore, the reactivity of the 4,0 isomer is peculiar compared to that of the other isomers, decreasing rapidly with side chain branching, while there is little effect of side chain branching for the other isomers (i.e., $k_{\text{TAc}}/k_{\text{TPiv}}$ is 4.74, 1.11, and 1.41 for the 4,0, 3,1, and cis 2,2 isomers); as well, the decrease in rate constant upon chain extension from TAc to TPro, where initial transannular side chain contact is first noted, is slightly greater for the 4,0 isomer (i.e., $k_{\text{TAc}}/k_{\text{TPro}}$ is 1.38, 1.18, 1.22, and 1.16 for the 4,0, 3,1, cis 2,2, and trans 2,2 isomers), consistent with a transannular effect. For the TPiv isomers, the behavior of 4,0 TPiv is unique. Although they exhibit the same isomer reactivity order as that noted for the other PFPs, 3,1, cis 2,2, and trans 2,2 TPiv metalate at rates similar to those of the corresponding TPro isomers while 4,0 TPiv metalates 3.4-fold times slower than 4,0 TPro. This comparison suggests that an indirect steric effect on reactivity is accentuated in the 4,0 isomer. Similar trends have been noted for the 4,0 PFP diacids which exhibit spectral blue shifts relative to those of the corresponding free bases while red shifts are reported for the diacids of the other atropisomers.^{41,61} The degree of spectral blue shift for free base 4,0 PFPs, indicative of the net phenyl-to-core resonance interaction and phenyl conformation in the ground state (see discussion below and Table VII), correlates roughly with the decreases in Cu(II) incorporation reactivities for the 4,0 isomer as a function of side chain bulk in DMF. The comparable steric effects of side chains in the non-4,0 isomers of TPiv and TPro, although of very different steric bulk, are consistent with different preferred side chain amide/phenyl ring conformations (i.e., β) for linear vs branched side chains.⁶²

These observations suggest that core rigidity is enhanced for the 4,0 isomer due to "transannular" steric interactions, resulting in elevated activation barriers for metalation. These transannular effects are most simply attributed to reduced degrees of freedom for side chain position, and hence phenyl ring conformation, resulting from four cofacial appendages in mutual steric contact. In the extreme case of steric congestion in 4,0 TPiv, "transannular" steric interactions must require nearly absolute perpendicularity between phenyl rings and the porphyrin core and the amide-phenyl

TABLE III: Cu(II) Incorporation Rate Constants for Selected PFPs in 9:1 DMF/Water^a

	$k_{\text{obs}}/[\text{Cu(II)}],$ $\text{M}^{-1} \text{ s}^{-1}$	(k_{rel})	$k_{\text{DMF/water}}/k_{\text{DMF}}$
4,0 TAc	7.21×10^{-4}	(9.61)	1.02
3,1 TAc	1.38×10^{-4}	(1.83)	1.96
cis 2,2 TAc	1.00×10^{-4}	(1.33)	2.15
trans 2,2 TAc	7.51×10^{-5}	(1.00)	3.01
4,0 THex	3.54×10^{-4}	(4.72)	0.93

^aData previously reported in ref 39.

ring dihedral angle may be forced to differ from that noted in PFPs with linear side chains.⁶² Thus, in the crystal structure of 4,0 TPiv as the Fe(III) imidazole derivative, the phenyl rings are nearly perpendicular to the porphyrin core ($\alpha \sim 90^\circ$).⁴⁴ In the other isomers, contact between side chains may be avoided by the phenyl rings tilting away from one another as they approach coplanarity with the porphyrin core (i.e., e.g. $60^\circ < \alpha < 120^\circ$) since they are generally not flanked on both sides by cofacial substituents, resulting in less rigid porphyrin cores relative to the 4,0 isomer. Stereoelectronic factors are discussed in more detail below.

Cu(II) Incorporation in 9:1 DMF/Water. The metalation results in 9:1 DMF/water reveal a smaller range of reactivities relative to DMF toward the TAc isomers (i.e., ranges are 9.6 and 28.5, respectively, see Table III) as expected for a sterically controlled process where the metalating complex in 9:1 DMF/water (e.g., $\text{Cu}(\text{H}_2\text{O})_6^{2+}$ or $\text{Cu}(\text{DMF})_2(\text{H}_2\text{O})_4^{2+}$) is smaller than that in DMF (e.g., $\text{Cu}(\text{DMF})_6^{2+}$ and $\text{Cu}(\text{DMF})_4(\text{H}_2\text{O})_2^{2+}$). Thus, more facile metalation is noted for the 3,1, cis 2,2, and trans 2,2 atropisomers in 9:1 DMF/water consistent with direct steric control of reactivity. Likewise, the same atropisomer order of reactivities is noted in both DMF and 9:1 DMF/water. The fact that 4,0 TAc and 4,0 THex metalate at nearly the same rates in either medium (i.e., $k_{9:1 \text{ DMF/water}}/k_{\text{DMF}}$ are 1.02 and 0.93, respectively) suggests that their metalation is not controlled by direct steric exclusion of Cu(II) in a bimolecular reaction and is consistent with stereoelectronically controlled metalation (i.e., variations in core rigidities) for the 4,0 atropisomer in homogeneous solution. The atropisomer order, sensitivities to side chain extension, and relative accelerations for 3,1, cis 2,2, and trans 2,2 TAc in 9:1 DMF/water further support steric exclusion of metal ions from the porphyrin center.

Apparent Basicities in 9:1 DMF/Water. Although metalation rates are influenced by direct steric effects and core rigidity effects, porphyrin basicities in substituted TPPs are solely influenced by core deformabilities which are related to indirect steric effects (i.e., the ortho and transannular effects). Equilibrium constants for core diprotonation of TPP and the TAc isomers, expressed in terms of "apparent $\text{p}K_a$ " values, $\text{p}K_{3,4}^{\text{app}}$, are displayed in Table IV. The apparent basicity of the TAc isomers is 50 times less than that measured for TPP and is attributed to reduced resonance interaction between the porphyrin core and the phenyl rings due to the *o*-acetamidophenyl substituents (i.e., the ortho effect). The much reduced basicity for the TAc isomers relative to TPP ($\text{p}K_a^{\text{app}} = 3.4$ vs 1.7, respectively) demonstrates the large reductions in core deformabilities resulting from *o*-acetamide substitution. The TAc isomers are equally basic toward core diprotonation in 9:1 DMF/water, as might be expected since, for the C_2 alkylamide side chains, transannular steric contact is impossible. Based on steric interactions which promote phenyl ring perpendicularity with respect to the porphyrin core, we would predict that the order of basicities or net deformabilities for the PFPs is 4,0 TAc > 4,0 THA > 4,0 TPiv and trans 2,2 > cis 2,2 \sim 3,1 > 4,0. The degree of red shift for the PFP dications relative to their corresponding free bases, which reflects the net increase in phenyl-to-core resonance stabilization upon core deformation and protonation, follows this order.⁴¹

Zn(II) Incorporation into the PFPs in DMF. The Zn(II) incorporation rates for the linear PFPs (as the perchlorate salt) can be compared to those reported for the TPiv derivatives in DMF (nitrate and acetate salts).³² The reactivity order for linear PFPs

(58) Testa, B. *Principles of Organic Stereochemistry*; Marcel Dekker, Inc.: New York, 1979.

(59) Eaton, S. S.; Eaton, G. R. *J. Am. Chem. Soc.* **1975**, *97*, 3660.

(60) Bonnet, J. J.; Eaton, S. S.; Eaton, G. R.; Holm, R. H.; Ibers, J. A. *J. Am. Chem. Soc.* **1973**, *95*, 2141.

(61) See Table IX.

(62) For further discussion and ¹H NMR data, see the supplemental material to this issue of this journal available on microfilm.

TABLE IV: Apparent Basicities for TPP and Selected PFPs in 9:1 DMF/Water^a

porphyrin	p <i>K</i> _{3,4} ^{app}
TPP	3.4
4,0 TAc	1.7
3,1 TAc	1.7
cis 2,2 TAc	1.7
trans 2,2 TAc	1.7

^a Concentration of acid is in large excess over porphyrin.

TABLE V: Zn(II) Incorporation Rate Constants for Selected PFPs in DMF^a

porphyrin	4,0	3,1	cis 2,2	trans 2,2
TAc	57.6 ± 1.4	22.0 ± 2.9	14.9 ± 0.4	8.00 ± 0.13
TPro	59.4 ± 2.7	22.2 ± 0.4	27.0 ± 0.7	12.7 ± 1.3
THex	84.6 ± 19.4	34.4 ± 1.7	15.2 ± 0.6	7.9 ± 0.3
THA	72.9 ± 5.3	16.9 ± 2.9	24.1 ± 5.3	5.22 ± 0.3

^a Values in M⁻¹ s⁻¹ × 10⁷; errors are the average deviation.

(4,0 > 3,1 ~ cis 2,2 > trans 2,2, see Table V) indicates a general steric control of reactivity for any particular chain length, as previously noted for Zn(NO₃)₂ incorporation into the TPiv isomers where reactivity was presumed to be controlled by direct steric factors.³² In contrast to the Cu(II) results, there is no clear chain length dependency of metalation rates with Zn(ClO₄)₂. The ranges of reactivity for the four isomers are larger for linear PFPs reacting with Zn(ClO₄)₂ (i.e., $k_{4,0}/k_{trans\ 2,2} = 7.2\text{--}14.0$) than are those reported for reaction of Zn(NO₃)₂ with the TPiv isomers ($k_{4,0}/k_{trans\ 2,2} = 1.9$), suggesting greater steric control of reactivity in the present study. Non-first-order behavior observed in the initial portion of the reaction for linear PFPs with Zn(ClO₄)₂ may be due to precomplexation between a metal ion and a porphyrin (an "incubation period") prior to metal ion incorporation (see Scheme I, step 1) similar to that proposed for Zn(OAc)₂ and the TPiv isomers³² and in other metalation studies^{59,60} or may be related to the instability of Zn(II) salts in DMF.⁶³ The differences in reaction for Zn(II) and Cu(II), differences noted as the Zn counterion is varied and complex rate trends for Zn(II) incorporation into the PFPs indicate the complexity of the Zn(II) incorporation reaction, anion participation, second-order behavior of the Zn(II) ion proposed in certain cases,⁶⁴ and a lack of knowledge of the solvated Zn(II) species present in solution further complicate interpretation of these data. Peculiar reactivity patterns have also been noted for Zn(II) incorporation into an *o*-amido-phenylporphyrin bearing charged side chains.³³ Smaller ranges of reactivity for the PFP isomers reacting with the perchlorate salts of Zn(II) as compared to those of Cu(II) ($k_{4,0}/k_{trans\ 2,2} = 7.23\text{--}14.0$ vs 24.1–71.1, respectively) indicate differing steric sensitivities for the two metal ion complexes in DMF. An effect of coordination geometry has been previously noted with Co(II) complexes.⁶⁵

¹H NMR Spectral Characteristics of the PFPs. The ¹H NMR resonance positions for selected protons of the PFPs (see Figure 3 for proton assignments) vary as a function of side chain length (see Table VI) and atropisomer structure.⁶²

Phenyl Ring Conformation (α). Crystal structures obtained for two *o*-amido-substituted TPPs, including the monoimidazole derivative of Fe(II), 4,0 TPiv, indicate an almost perpendicular dihedral angle, α, between the ortho-substituted phenyl rings and the macrocyclic core,^{43,45} while a 40° dihedral angle has been estimated for TPP in solution.⁵¹ A measure of the time-averaged value of α is best obtained by comparing H_a phenyl resonances in the 4,0 isomers, since they are located in an area of relatively high magnetic field anisotropy and lie on a face bearing no al-

TABLE VI: Chemical Shifts (ppm) for Selected Protons of the 4,0 PFPs in CDCl₃: H_a, Amide N–H, β-Pyrrole, and Pyrrole N–H

	β-pyrrole	phenyl H _a	amide N–H	pyrrole N–H
TPP	8.82 (s)	8.20 (dd)		-2.78 (s)
TAc	8.84 (s)	8.69 (d)	6.80 (s)	-2.77 (s)
TPro	8.83 (s)	~8.75 (d)	6.87 (s, br)	-2.78 (s)
TBu	8.83 (s)	8.77 (d)	6.87 (s, br)	-2.77 (s)
THex	8.83 (s)	8.77 (d)	6.85 (s)	-2.77 (s)
THept	8.83 (s)	8.77 (d)	6.85 (s, br)	-2.77 (s)
TOct	8.84 (s)	8.76 (d)	6.87 (s, br)	-2.77 (s)
TDec	8.84 (s)	8.78 (d)	6.85 (s, br)	
THA	8.83 (s)	8.78 (d)	6.83 (s, br)	-2.78 (s)
TiBu	8.87 (s)	8.78 (d)	7.01 (s)	-2.73 (s)
TPiv	8.80 (s)	8.70 (d)	7.18 (s)	-2.61 (s)

ylamide substituents.⁶⁶ Taking the difference in chemical shift for a proton on benzene (7.27 ppm) from that of the meta proton on the model compound acetanilide (*N*-phenylacetamide, 7.27 ppm)⁶⁷ as the correction for *o*-amide substitution in the PFPs relative to TPP and noting that there is relatively weak phenyl-to-core resonance interaction,¹³ the chemical shift for H_a in TPP and the 4,0 PFPs can be compared directly. The general downfield shift noted for H_a upon side chain extension, exhibiting the largest change between TPP and 4,0 TAc (i.e., Δδ = 0.49 ppm; see Table VI) and smaller subsequent changes for 4,0 TPro and 4,0 THA (i.e., Δδ = 0.06 and 0.03 ppm, respectively), can be attributed to a continuous, attenuating change in phenyl ring conformation with increasing ortho-substituent length, i.e., α approaches 90°. Furthermore, the pattern of chemical shifts for the linear PFPs as compared to TPP suggest that the proposed conformational change for the porphyrin free base in solution is induced primarily by steric interactions between the ortho substituent and β-pyrrole protons (i.e., the greatest effect is noted at short chain lengths) rather than transannular steric interactions between cofacial side chains (i.e., significant only at longer chain lengths). The NMR data are interpreted to mean that in the ground state, at least in the CDCl₃ solution, the relative degrees of phenyl ring–porphyrin core perpendicularity follow the order TPP << 4,0 TAc < 4,0 TPro < 4,0 TBu–4,0 THA. Relative Cu(II) incorporation rate constants in DMF for these compounds follow the exact opposite order (see Table I), suggesting that resonance interaction between the phenyl rings and porphyrin core occurs during metalation for these compounds whose reactivity differences are solely determined by deformability factors (see Tables II and VIII). Changes in the porphyrin π system, evidenced in UV–visible absorption spectral shifts and severe side chain conformational changes (i.e., changes in β indicated by unusual amide N–H and side chain methyl shifts), complicate interpretation of the anomalous H_a resonance position for 4,0 TPiv. Conformational differences for 4,0 PFPs bearing bulky side chains are addressed in detail in terms of pseudoparallel or -perpendicular *s*-trans side chain amide orientations (i.e., variations in the angle, β) elsewhere.⁶² Overall, evidence for orientational differences for undeformed PFPs in solution, attributable primarily to side chain–β-pyrrole steric interactions, suggest that an inherent tendency for phenyl ring perpendicularity should persist upon core deformation (i.e., during metalation).

The strong induced magnetic field of the porphyrin nucleus results in significant anisotropic effects on the PFP side chain resonances resulting in chemical shift differentiation as a function of atropisomer (i.e., see Figure 5) and side chain structure.⁶² The aliphatic side chain resonances of the THex isomers are separately resolved, as shown in Figure 5. In general, the 3,1 isomer exhibits three types of side chain resonances similar to those of the other three atropisomers. The methyl resonances of 3,1 TAc are not

(63) A reviewer has noted that Zn(II) salts may form metastable solutions in DMF.

(64) Proposed metal ion complexation on one face and assistance from a second metal ion on the opposite face is discussed in: Robinson, L. R.; Hambright, P. *Inorg. Chim. Acta* 1991, 185, 17.

(65) Phillips, J. N. *Rev. Pure Appl. Chem.* 1959, 9, 257.

(66) Information concerning phenyl ring conformation cannot be readily obtained for non-4,0 PFPs nor from resonance positions of other protons since β-pyrrole resonances are relatively insensitive to changes in phenyl ring orientation (range: 0.07 ppm) while the other aromatic protons are either relatively insensitive or additionally affected by amide substitution and conformational changes in the amide substituents.

(67) Pouchert, C. J. *The Aldrich Library of NMR Spectra*, 2nd ed.; Aldrich Chemical Co., Inc.: Milwaukee, WI, 1983; Vol. 2, p 334.

TABLE VII: Absorption Maxima and Soret Bandwidths for the PFP Free Bases in DMF^a

porphyrin	Soret ($W_{1/2}$)	IV	III	II	I	$\Delta\lambda_{\text{Soret}}$	$\Delta\lambda_{\text{Vis}}$
TPP	417.2 (11.8)	513.6	548.0	590.0	645.6	0.0	0.0
4,0 TAc	422.8 (14.2)	517.6	550.8	592.4	648.4	+5.6	+12.0
3,1 TAc	423.6 (14.0)	517.6	551.6	592.4	648.0	+6.4	+12.4
cis 2,2 TAc	424.0 (14.1)	517.6	551.2	592.4	648.8	+6.8	+12.8
trans 2,2 TAc	423.6 (14.1)	518.0	552.0	592.8	648.0	+6.4	+13.6
4,0 TPro	423.2 (14.1)	517.6	551.2	592.8	647.6	+6.0	+12.0
3,1 TPro	424.0 (14.2)	518.0	552.4	592.8	648.4	+6.8	+14.4
cis 2,2 TPro	424.0 (14.1)	518.0	552.4	592.8	648.4	+6.8	+14.4
trans 2,2 TPro	424.8 (14.6)	518.8	553.6	593.6	650.0	+7.6	+18.8
4,0 TBu	422.8 (14.2)	517.2	550.4	592.0	648.8	+5.6	+11.2
4,0 THex	423.2 (14.0)	517.2	551.2	591.6	647.6	+6.0	+10.4
3,1 THex	424.4 (14.1)	518.4	552.0	592.8	648.0	+7.2	+14.0
cis 2,2 THex	424.4 (14.2)	518.0	552.4	592.8	648.8	+7.2	+14.8
trans 2,2 THex	424.8 (14.6)	518.8	553.2	593.2	649.6	+7.6	+17.6
4,0 THA	423.2 (14.0)	517.2	551.2	592.4	647.6	+6.0	+13.2
3,1 THA	423.6	518.4	549.2	592.8	649.2	+6.4	+12.4
cis 2,2 THA	424.4 (14.1)	518.4	552.4	593.2	648.4	+7.2	+15.2
trans 2,2 THA	424.8 (14.4)	518.8	553.2	593.2	649.2	+7.6	+17.2
4,0 TiBu	422.8 (14.4)	517.2	550.8	592.4	648.0	+5.6	+11.2
4,0 TPiv	419.6 (15.9)	514.4	546.4	589.6	644.4	+2.4	-2.4
3,1 TPiv	422.8 (16.1)	517.6	551.2	593.2	649.2	+5.6	+14.0
cis 2,2 TPiv	422.4 (17.8)	517.6	551.6	592.8	648.8	+5.2	+13.6
trans 2,2 TPiv	426.0	521.2	556.4	596.4	652.4	+8.8	+29.2

^a All values given in nm. ^b $\Delta\lambda_{\text{Soret}} = \lambda_{\text{PFP}} - \lambda_{\text{TPP}}$. ^c $\Delta\lambda_{\text{Vis}} = (\lambda^{\text{IV}} + \lambda^{\text{III}} + \lambda^{\text{II}} + \lambda^{\text{I}})_{\text{PFP}} - (\lambda^{\text{IV}} + \lambda^{\text{III}} + \lambda^{\text{II}} + \lambda^{\text{I}})_{\text{TPP}}$.

resolved. The effect of steric interactions between side chains is clearly indicated by the chemical shift positions of the terminal methyl resonances since the degree of shielding observed increases as the number of cofacial side chains increases for any particular side chain (terminal methyl resonances in ppm are 4,0 (0.47 (t)); 3,1 (0.51 (m, 3 H), 0.45 (m, 6 H), 0.25 (t, 3 H)); cis 2,2 (0.35 (t)); and trans 2,2 THex (0.28 (t)). The 3,1 isomer exhibits a lone terminal methyl resonance which is even more shielded than that for the trans 2,2 isomer since it is the most free to penetrate the shielding cone of the porphyrin core.

Absorption Spectral Behavior of the PFPs. UV-visible spectral differences for the PFP free bases in homogeneous solution are smaller in magnitude than those of the porphyrin diacids (range of total diacid visible band I and II shifts for the PFPs as compared to TPP are +11–42 nm⁴¹ as opposed to -2.4 to +29.2 nm for the four free base bands, see Table VII). UV-visible absorption spectra of the PFPs generally exhibit hyperchromic shifts in both the Soret and visible bands in DMF ($\lambda_{\text{Soret}} = 419.6$ –426.0 nm) relative to TPP ($\lambda_{\text{Soret}} = 417.2$ nm). Soret bandwidths are broader for the PFPs than for TPP ($W_{1/2} = 14.0$ –17.8 vs 11.8 nm, respectively) and are broader and more varied for the TPiv isomers than with the other PFPs ($W_{1/2} = 15.9$ –17.8 nm vs 14.0–14.6 nm, respectively).

Steric interactions between the alkylamide side chains and the porphyrin π system have been proposed by Corwin et al. as the source of the spectral red shift observed upon ligand binding to metalloporphyrins.⁶⁸ Steric interactions between the side chains and the porphyrin chromophore affect the more diffuse porphyrin π antibonding levels more strongly than the ground-state levels and are proposed to result in a general red shift for the PFPs relative to TPP. This red shift offsets the blue shift expected on the basis of reduced phenyl-to-core resonance in the PFPs. Shielding of side chain proton resonances in ¹H NMR spectra and carbonyl orientations placing side chains over the porphyrin core⁶² suggest that the side chains should encounter steric contact with the porphyrin π system. Absorption spectral shifts in the trans 2,2 isomer, where "transannular" steric interactions are minimized, can be taken as a measure of side chain/ π -system interactions. These interactions can account for the Soret red shift with increasing side chain bulk in the trans 2,2 isomer ($\lambda_{\text{Soret}}^{\text{trans 2,2}} = 423.6, 424.8, \text{ and } 426.0$ nm for TAc, TPro–THA, and TPiv). A similar trend is noted in the visible band shifts ($\Delta\lambda_{\text{Vis}}^{\text{trans 2,2}} = 13.6, 17.2$ –18.8, and 29.2 nm for TAc, TPro–THA, and TPiv).

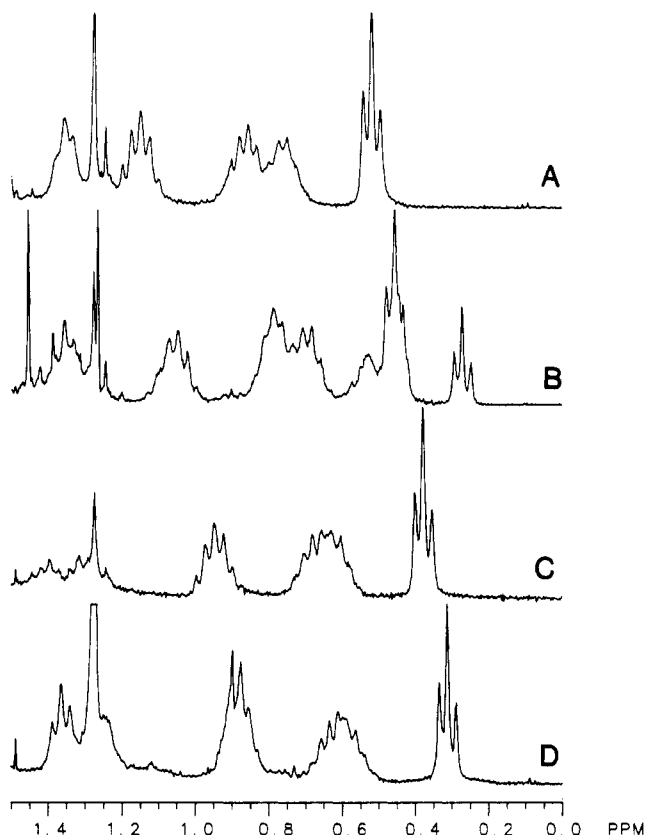


Figure 5. Aliphatic ¹H NMR resonances for the THex isomers in CDCl₃: (A) 4,0 THex; (B) 3,1 THex; (C) cis 2,2 THex; (D) trans 2,2 THex.

The hypsochromic shift in electronic absorption spectra of free base 4,0 TPiv relative to the other TPiv atropisomers has been attributed to an "electronic effect" by Hatano and Anzai.⁶⁹ This rather loosely defined electronic effect follows an order of 4,0 < 3,1 ~ cis 2,2 < trans 2,2 in terms of reduced metalation reactivities for 4,0 TPiv.³² We have noted that all free base 4,0 PFPs exhibit blue shifts in absorption spectra relative to the other isomers (see Table VII). The magnitude of the observed blue shifts for the 4,0 versus the corresponding trans 2,2 isomer generally increases with increasing side chain bulk (compare $\Delta\lambda_{\text{Soret}}$ and $\Delta\lambda_{\text{Vis}}$ for

(68) Corwin, A. H.; Whitten, D. G.; Baker, E. W.; Kleinspehn, G. G. *J. Am. Chem. Soc.* 1963, 85, 3621.

(69) Anzai, K.; Hatano, K. *Chem. Pharm. Bull.* 1984, 32, 1273.

TABLE VIII: Rate Reduction Factors Attributed to Direct Steric Effects^a

H ₂ P	<i>n</i>	<i>k</i> (0, <i>n</i>) _{est}	<i>k</i> (1, <i>n</i>) _{est}	<i>k</i> (2, <i>n</i>) _{adj}	<i>k</i> (2, <i>n</i>) _{opp}	<i>k</i> (3, <i>n</i>) _{est}	<i>k</i> (4, <i>n</i>) _{est}
DMF							
TPP	0	1.0					
TAc	2	1.0	10.9	30.4	56.8	140	649
TPro	3	1.0	12.9	37.1	66.1	168	761
THex	6	1.0	24.9	76.5	239	680	5900
THA	16	1.0	37.3	130	310	992	7600
TPiv	tBu	1.0	11.9	42.9	54	206	621
9:1 DMF/Water							
TAc	2	1.0	5.99	14.3	19.0	38.0	101

^a Calculated using values in Table II by dividing *k*(0,2) by *k*(*a*,*n*), a particular facial metalation rate constant. Values indicate the rate reduction factor relative to *k*(0,0) (in TPP) attributable to direct steric effects.

TABLE IX: Net Visible Band Absorption Spectral Shifts for TPP and the PFP Diacids in Solution^a

porphyrin	<i>n</i>	net spectral shift, nm				<i>o</i> -phenyl/ β -pyrrole shift $\Delta\lambda_{\text{TPP}} - \Delta\lambda_{\text{t},2,2}$	transannular shift $\Delta\lambda_{\text{t},2,2} - \Delta\lambda_{4,0}$
		$\Delta\lambda_{4,0}$	$\Delta\lambda_{3,1}$	$\Delta\lambda_{\text{cis},2,2}$	$\Delta\lambda_{\text{trans},2,2}$		
TPP	0			+30			
TPro	3	-2	+10	+11	+22	8	24
THA	16	-3	+11	+7	+15	15	18
TPiv	tBu	-10	+3	+4	+10	20	20

^a Taken from ref 41. Shifts are $\lambda_{\text{diacid}} - \lambda_{\text{free base}}$. Spectra recorded in benzene; diacids are the dihydrochloride salts.

4,0 and trans 2,2 isomers in Table VII); thus, 4,0 TPiv exhibits the greatest blue shift, and 4,0 TAc the least, and 4,0 TPiv exhibits blue-shifted absorption relative to 4,0 TAc. The blue shift for the 4,0 isomer is attributed to reduced phenyl-to-core resonance—larger values of the dihedral angle, α , as discussed above (see Figure 3)—due to steric interactions between cofacial side chains.

Similarly, variations in the degree of phenyl-to-core resonance in core-deformed PFPs are reflected in different net absorption spectral shifts ($\Delta\lambda$) for the visible bands of the corresponding PFP diacids relative to that observed for the TPP diacid, H₂TPP²⁺.⁶¹ Blue shifts and reduced red shifts for the PFP dications have been explained by a change in the preferred phenyl ring conformation. The generally reduced red shift in the PFPs relative to TPP is attributed to reduced phenyl-to-core resonance, and the atropisomer order of spectral shifts (i.e., trans 2,2 > cis 2,2 > 3,1 > 4,0) is attributed to cofacial transannular steric interactions in the free bases and magnified in the porphyrin dications. Accordingly, the observed diacid red shifts decrease for all four PFP atropisomers with increasing side chain bulk. Hence, for the porphyrins, basicities must correlate strongly with core deformabilities and, for substituted TPPs, phenyl-to-core resonance stabilization of the diacids is a function of transannular steric interactions and side chain bulk. Furthermore, the fact that thermal equilibrium isomeric ratios for the free base porphyrins (e.g. 4,0 (4%):3,1 (47%):cis 2,2 (29%):trans 2,2 (20%) for the THA isomers as compared to the statistical distribution 12.5:50:25:12.5% respectively) are skewed in favor of the trans 2,2 isomer for the porphyrin dications (3, 37, 27, and 33%, respectively)⁴¹ indicates that core deformation permits enhanced steric interactions between adjacent side chains and restricts phenyl ring conformation (α). As suggested from the PFP diacid spectral shifts, on the average, the phenyl rings of a core-distorted tetraphenylporphyrin should be restricted to a more vertical arrangement ($\alpha \rightarrow 90^\circ$) as ortho-substituent bulk increases due to both transannular sterically induced rigidity in the 4,0, 3,1, and cis 2,2 isomers and *o*-phenyl/ β -pyrrole-induced rigidity. Core rigidities are reflected in the metalation data.

The shifts in the Soret and visible bands relative to TPP are most varied in the TPiv isomers (i.e., for the 4,0, 3,1, cis 2,2, and trans 2,2 isomers, $\Delta\lambda_{\text{Soret}} = 2.4, 5.6, 5.2,$ and 8.8 nm; $\Delta\lambda_{\text{vis}} = -2.4, 14.0, 13.6,$ and 29.2 nm, respectively) as expected on the basis of side chain bulk. In no case does the transannular-induced blue shift for the 4,0 isomer exceed the side chain/ π -system induced red shift relative to TPP; for 4,0 TPiv, $\Delta\lambda_{\text{Soret}} = +2.4$ and $\Delta\lambda_{\text{vis}} = -2.4$ nm. Changes in electronic energy levels are attributed to (1) steric interactions between alkylamidophenyl substituents and the porphyrin π system⁶⁸ (resulting in net red shifts for the

PFPs relative to TPP), (2) changes in preferred phenyl conformation (larger values of α reducing phenyl-to-core conjugation resulting in additional blue shifts), and possibly (3) differing electronic effects caused by changes in side chain conformation (i.e., $25 > \beta > 120^\circ$).⁶² Conformational differences for the free base PFPs, as reflected in differing absorption spectral properties, should be magnified during metalation in transition states and intermediates in which core deformation permits greater phenyl-to-core resonance yet as limited by PFP atropisomer and side chain structure.

Separation of the Two Types of Stereoelectronic Effects

Estimation of the Magnitude of the Ortho Effect and Transannular Effect on Core Reactivities. Identical $\text{p}K_{3,4}$ values and the lack of side chain steric contact for the TAc isomers (by ¹H NMR spectroscopy and molecular models) allow us to approximate the stereoelectronic factors due to ortho substituent/pyrrole steric interactions as compared to TPP as equal to the ratio of facial metalation rate constants for TPP and 4,0 TAc (i.e. $k(0,0)/k(0,2) = 28.3$). Since the reduced facial metalation rate constant for the unsubstituted face of the other 4,0 isomers is a product of both stereoelectronic effects (i.e., ortho substituent/pyrrole interaction and transannular steric interactions) discussed above, transannular stereoelectronic reductions in core reactivity can be calculated for the 4,0 atropisomers. These (calculated as follows: $k(0,0)/28.3[k(0,n)] = \sim k_{4,0\text{TAc}}/k_{4,0\text{PFP}}$) are 4,0 TAc (1.0), 4,0 TPro (1.4), 4,0 THex (1.9), 4,0 THA (2.2), 4,0 TiBu (2.2), and 4,0 TPiv (4.8). These values are approximate since the ortho effect may actually increase with increasing substituent size, as suggested by an increasing effect of side chain bulk on spectral shifts for the trans 2,2 isomer relative to TPP ($\Delta\lambda_{\text{TPP}} - \Delta\lambda_{\text{trans},2,2} = 8, 15,$ and 20 nm for TPro, THA, and TPiv, respectively) and significant additional shifts for a structural change to the 4,0 atropisomer ($\Delta\lambda_{\text{trans},2,2} - \Delta\lambda_{4,0} = 24, 18,$ and 20 nm for TPro, THA, and TPiv, respectively).

Estimation of Direct Steric Effects. Direct steric effects for any particular PFP face can be estimated by dividing *k*(0,2), the facial metalation rate constant for the unsubstituted face of 4,0 TAc which accounts for the effects of ortho substituent/pyrrole stereoelectronically induced core rigidity (since steric interactions between side chains are impossible in the TAc isomers), by any individual facial metalation rate constant; this analysis assumes that transannular steric effects are minimal for non-4,0 PFPs and that the ortho effect is relatively constant regardless of side chain bulk. The data in Table VIII, indicating the magnitude of direct steric effects on exclusion of Cu(II), reveal that direct steric effects, which account for up to a 7600-fold rate reduction relative to *k*(0,0) for TPP, can be much larger than the product of indirect

steric effects (stereoelectronic effects), which is at best 135 (i.e., $k(0,0)/k(0,tBu)$).

Mechanistic Implications for Cu(II) Incorporation into the PFPs. Prior studies of PFP metalation in homogeneous solution have noted that steric effects, alone, can account for only a small portion of the reduction in reactivity toward Cu(II) observed for the PFPs as compared to the parent compound, TPP.²⁷ A particularly intriguing aspect of metal ion incorporation with the tetraarylporphyrins is the interplay of side chain sterics, phenyl ring-core conformation and core deformability. Steric shielding about one macrocyclic face has been employed to stabilize ortho-substituted Fe(II) TPPs which reversibly bind oxygen^{39,70} while steric interactions between cofacial side chains have been cited as responsible for nonstatistical equilibrium isomer ratios of the picket fence porphyrins which undergo thermal atropisomerization at elevated temperatures.⁴¹ Porphyrin core conformation has been studied in terms of distortion from planarity by X-ray crystallography^{48,49,52,57,71} and core deformabilities in solution by thermal and photoatropisomerization studies.⁴¹ Yet, in many instances, the peculiar behavior of ortho-substituted derivatives^{16,22,26,32,33,69,72,73} has not been attributed to an inherent inability to attain a coplanar phenyl ring-porphyrin core geometry following core deformation due to steric interactions between the ortho substituent and the β -pyrrole hydrogen atoms, that such may, in fact, be the case is implicated in studies of PFP atropisomerization, spectral studies of the PFP dications,⁴¹ and the present investigations.

A generally accepted mechanism for porphyrin metalation in homogeneous solution, accounting for observations from a wide variety of studies, is shown in Scheme 1. Outer-sphere complexation (i.e., step 1) has been suggested in a number of studies from a kinetic scheme including a preequilibrium expression for free base porphyrin-metal ion association.^{74,75} Studies of predeformed porphyrins, such as free base porphyrins precomplexed to certain hydrogen bond donors (via pyrrole N-H bonding to *p*-nitrophenol)^{76,77} and various investigations of *N*-methyl TPPs,^{19,78} suggest that porphyrin core deformation accelerates metalation; catalytic metalation by large, nonincorporating metal ions⁷⁹ and accelerated incorporation of Zn(II) into out-of-plane metallo-TTP complexes (i.e., transmetalation) as compared to its direct incorporation into free base TPP^{80,81} further implicate porphyrin core deformation during the metalation process (i.e., step 2 and/or steps 3 and 4).⁸² The sequential formation of metal-nitrogen bonds by desolvation/ligation steps where one such step is rate limiting or more than one step is competitive (i.e., steps 3 and 4) is supported by a correlation between solvent exchange rates from the metalating complex and metalation rate constants.^{2,78,83} An inverse first- or inverse second-order dependence of metalation rate on hydrogen ion concentration^{18,29,54-56} reveals that both central porphyrin N-H protons of the free base (H_2P) are retained in the rate-determining step(s), but that formation of the porphyrin mono acid (H_3P^+) or diacid (H_4P^{2+}) retards metalation (see Steps 3-5).

The major factors governing Cu(II) incorporation rate constants in the series of ortho-substituted TPPs in this study are (1) facial steric effects and (2) porphyrin core deformabilities, which may be reflected in core deformation and conformational alterations in the ground state. Physical and physicochemical properties of the PFPs differ from those of porphyrins not bearing meso-aryl substituents. *meso*-Phenyl substitution results in (1) more ruffled porphyrin cores for the TPPs as compared to natural porphyrins according to X-ray crystallography⁸⁴⁻⁸⁷ permitting greater resonance interaction between phenyl rings and the porphyrin core and (2) red shifts in electronic absorption spectra of both the porphyrin free bases and the diacids in solution due to phenyl ring-porphyrin core conjugation (porphine $\lambda_{max} = 395$ nm (benzene); TPP $\lambda_{max} = 419$ nm (benzene)).⁸⁸ Such resonance interactions for para-substituted TPPs are demonstrated by correlations of substituent effects with pyrrole N-H stretching frequencies⁸⁹ and IR vibrations in substituted cobalt porphyrins⁵¹ while UV-visible spectral shifts for para-substituted TPPs correlate more strongly to resonance (80%) substituent effects than to inductive effects (20%).⁹⁰ The observation of such core deformation and apparent conformational variation in the ground state suggests that these structural effects may be enhanced upon core deformation (e.g., during the metalation process) as suggested herein.

Various properties of the PFPs indicate that two types of steric interactions, as elucidated above (see Stereoelectronic Effects on Cu(II) Incorporation), are present, which should have a direct bearing on phenyl ring conformation. Many ortho-substituted TPPs form rotationally stable atropisomers.^{27,29,33,40,41,43,45,47,53,91-103} Atropisomerization activation energies reflect the degree of steric contact between ortho substituents and β -pyrrole hydrogen atoms ($\Delta G^*_{atrop} = 15.6-17.9, 29.1, 29.1, \text{ and } 30.5$ kcal/mol for non-ortho-substituted metallo-TTPs,^{59,60} 4,0 TPro, 4,0 THA, and 4,0 TPiv,⁴¹ respectively), hence the expected order of the dihedral angles, α . The "ortho effect" is evident in the consequences of ortho substitution on TPP basicities and metalation reactivities,^{16,26,33,104,105} spectral shifts,^{41,84} and atropisomerization bar-

(84) Gottwald, L. K.; Ullman, E. F. *Tetrahedron Lett.* **1969**, *36*, 3071.

(85) Fleischer, E. B. *Acc. Chem. Res.* **1970**, *3*, 105.

(86) Collins, D. M.; Hoard, J. L. *J. Am. Chem. Soc.* **1970**, *92*, 3761.

(87) Hoard, J. L. *Ann. N. Y. Acad. Sci.* **1973**, *206*, 18.

(88) Smith, K. M., Ed. *Porphyrins and Metalloporphyrins*; Elsevier: Amsterdam, 1975; p 876.

(89) Alben, J. O.; Choi, S. S.; Adler, A. D.; Caughey, W. S. *Ann. N. Y. Acad. Sci.* **1973**, *206*, 278.

(90) Thomas, D. W.; Martell, A. E. *Arch. Biochem. Biophys.* **1958**, *76*, 286.

(91) Dirks, J. W.; Underwood, G.; Matheson, J. C.; Gust, D. *J. Org. Chem.* **1979**, *44*, 2551.

(92) Crossley, M. J.; Field, L. D.; Forster, A. J.; Harding, M. M.; Sternhell, S. *J. Am. Chem. Soc.* **1987**, *109*, 341.

(93) Walker, F. A.; Avery, G. L. *Tetrahedron Lett.* **1971**, *52*, 4949.

(94) Buckingham, D. A.; Gunter, M. J.; Mander, L. N. *J. Am. Chem. Soc.* **1978**, *100*, 2899.

(95) Lexa, D.; Maillard, P.; Momenteau, M.; Saveant, J.-M. *J. Am. Chem. Soc.* **1984**, *106*, 6321.

(96) Collman, J. P.; Brauman, J. I.; Collins, T.; Iverson, B. L.; Lang, G.; Pettman, R. B.; Sessler, J. L.; Walters, M. A. *J. Am. Chem. Soc.* **1983**, *105*, 3038.

(97) Sanders, G. M.; van Dijk, M.; van Veldhuizen, A.; van der Plas, H. C.; Hofstra, U.; Schaafsma, T. J. *J. Org. Chem.* **1988**, *53*, 5272.

(98) Young, R.; Chang, C. K. *J. Am. Chem. Soc.* **1985**, *107*, 898.

(99) Cole, G. M., Jr.; Doll, D. W.; Holt, S. L. *J. Am. Chem. Soc.* **1983**, *105*, 4477.

(100) Hatano, K.; Anzai, K.; Kubo, T.; Tamai, S. *Bull. Chem. Soc. Jpn.* **1981**, *54*, 3518.

(101) Mansuy, D.; Battioni, P.; Renaud, J.-P.; Guerin, P. *J. Chem. Soc., Chem. Commun.* **1985**, 155.

(102) Eshima, K.; Makoto, Y.; Nishide, H.; Tsuchida, E. *J. Chem. Soc., Chem. Commun.* **1985**, 130.

(103) Hatano, K. *Chem. Pharm. Bull.* **1985**, *33*, 4116.

(104) Meot-Ner, M.; Adler, A. D. *J. Am. Chem. Soc.* **1975**, *97*, 5107.

(105) Adler, A. D. *Ann. N. Y. Acad. Sci.* **1973**, *206*, 7.

(70) Collman, J. P. *Acc. Chem. Res.* **1977**, *10*, 265.

(71) Fleischer, E. B.; Miller, C. K.; Webb, L. E. *J. Am. Chem. Soc.* **1964**, *86*, 2342.

(72) Hambright, P.; Gore, T.; Burton, M. *Inorg. Chem.* **1976**, *15*, 2314.

(73) Anzai, K.; Hosokawa, T.; Hatano, K. *Chem. Pharm. Bull.* **1986**, *34*, 1865.

(74) Funahashi, S.; Yamaguchi, Y.; Tanaka, M. *Bull. Chem. Soc. Jpn.* **1984**, *57*, 204.

(75) Pasternack, R. F.; Vogel, G. C.; Skowronek, C. A.; Harris, R. K.; Miller, J. G. *Inorg. Chem.* **1981**, *20*, 3763.

(76) Guilleux, L.; Krausz, P.; Nadjo, L.; Uzan, R. *J. Chem. Soc., Perkin Trans. 2* **1985**, 951.

(77) Guilleux, L.; Krausz, P.; Nadjo, L.; Uzan, R.; Gianotti, C. *J. Chem. Soc., Perkin Trans. 2* **1984**, 475.

(78) Bain-Ackerman, M. J.; Lavalley, D. K. *Inorg. Chem.* **1979**, *18*, 3358.

(79) Tanaka, M. *Pure Appl. Chem.* **1983**, *55*, 151. Compare to: Adeyemo, A.; Krishnamurthy, M. *Inorg. Chem.* **1977**, *16*, 3355.

(80) Reid, J.; Hambright, P. *Inorg. Chim. Acta* **1979**, *33*, L135.

(81) Grant, C., Jr.; Hambright, P. *J. Am. Chem. Soc.* **1969**, *91*, 4195.

(82) Pasternack, R. F.; Sutin, N.; Turner, D. H. *J. Am. Chem. Soc.* **1976**, *98*, 1908.

(83) Hambright, P.; Chock, P. B. *J. Am. Chem. Soc.* **1974**, *96*, 3123.

riers.^{41,59,84,91-93,100} Metalation trends for substituted TPPs in DMF also reflect electronic properties of the phenyl substituents.²⁶ Reduced Cu(II) incorporation rates reported for *meso*-tetrakis(*o*-ethoxyphenyl)porphyrin, for which four moderately stable ($\Delta G^{\ddagger}_{\text{atrop}} = 25.9$ kcal/mol) for the tetramethoxy derivative) atropisomers exist in solution,⁹¹ and for *meso*-tetrakis(*o*-methylphenyl)porphyrin,²⁶ as compared to their para-substituted counterparts, indicate a profound effect of ortho vs para substitution.

A combination of steric and deformability effects may play a variety of specific roles during the metalation process. First, steric effects, restricting collisions between metal ion and the porphyrin core, are probably only partially responsible for the atropisomer order of reactivities. Intermediates A and B (see steps 3 and 4, Scheme 1) should be destabilized by steric interactions between side chains and ligated metal ion in the 3,1, *cis* 2,2, and *trans* 2,2 isomers. Increasing facial steric effects as atropisomer structure is varied (i.e., 4,0 \rightarrow *trans* 2,2) and side chain bulk increases should reduce the net k_{obs} calculated from Scheme 1 by primarily decreasing K_{OS} (i.e., if step 5 is rate determining, $k_{\text{obs}} = K_{\text{OS}}K_{\text{deform}}K_1K_2k_3$). For steps 2-4, which involve increases in core deformation, side chain/metal ion steric interactions should decrease upon core deformation as the phenyl rings approach coplanarity with the porphyrin core as in the porphyrin diacid (see Figure 4). For the 4,0 isomer, direct steric effects should be irrelevant assuming that metalation occurs from only the unsubstituted face. In one report, Cu(II) metalation of 4,0-*meso*-tetrakis(*o*-maleamoylphenyl)porphyrin, which possesses a tetracarboxylate coordination pocket, in 1:1 DMF/water is extremely rapid²⁹ and suggests that relatively rapid carboxylate-catalyzed insertion (i.e., anionic electrostatic catalysis, as noted at anionic interfaces)³⁹ is possible from the more hindered porphyrin face. Reduced steric discrimination in this case can be attributed to an aquo copper complex (as opposed to the bulky $\text{Cu}(\text{DMF})_6^{2+}$) and to side chain ligation to Cu^{2+} ($K_{\text{assoc}} = 1.5 \times 10^3 \text{ M}^{-1}$).

Core deformability effects as present in the core-deformed PFP diacids⁴¹ should be significant for intermediates A and B. Energetic differences between the PFP diacids, based on equilibrium thermodynamic data,⁴¹ can be attributed to (1) sterically limited side chain mobility and (2) a net reduction in resonance between the porphyrin core and phenyl rings, particularly in the 4,0 PFPs. Due to similarities in the porphyrin diacid and intermediate B (i.e., see Figure 4), these same factors should destabilize intermediates A and B in terms of core deformabilities, thereby reducing metalation rates. The effects of deformability restrictions should be felt throughout the reaction coordinate from initial core deformation to final product. From Scheme 1, it is apparent that core deformability differences should influence steps 2 and 3 and, to a lesser extent, step 4 since the porphyrin core undergoes the most significant core deformation in step 3; therefore the most salient effect of core deformabilities on k_{obs} should be noted by reductions in K_{deform} , K_1 , and K_2 . Although, for the PFPs studied, the significance of core deformation is relatively small (there is, at most, a 4.7-fold reduction in reactivity for 4,0 TPiv relative to 4,0 TAc), in the context of TPPs in general, the effect of reduced core deformabilities on Cu(II) incorporation rates are noteworthy (up to a 135-fold reduction).

A basicity-reactivity correlation often noted in porphyrin metalation reactions^{31,106} has previously been discussed in terms of Lewis basicities rather than in the context of porphyrin core deformabilities (deformation is required for core protonation of the free base porphyrin due to steric constraints of the central cavity). In this regard, an associative metalation mechanism¹⁰⁶ has, in general, been abandoned in favor of a dissociative mechanism, in which metal-to-nitrogen bonding occurs following a significant degree of ligand dissociation, based on a good correlation between solvent exchange rates of various metal ions and their metalation reactivities^{2,5,12,38,78,83,107} and other observations.^{26,83}

We suggest that the involvement of core deformation, as proposed from other studies where independent core deformation accelerates metalation,^{76,77,79,80,82,87,108,109} can account for the generally observed basicity-reactivity correlation. Correlations between reduction potentials and porphyrin metalation rates are consistent with this interpretation.^{21,22} The compensation effect for porphyrin metalation, where increases in ΔH^{\ddagger} are offset by corresponding decreases in ΔS^{\ddagger} , has been noted for Cu(II) incorporation into a variety of porphyrins including many ortho- and para-substituted TPPs in DMF²⁶ and natural porphyrins in ethanol.¹¹⁰ In general, higher activation enthalpies for ortho-substituted TPPs (23.8-24.9 kcal/mol) than for non-ortho-substituted TPPs (12.0-16.0 kcal/mol) and activation enthalpies for Zn(II) and Cd(II) incorporation into *N*-etioporphyrin III, which are both 5 kcal/mol greater than those of incorporation into *N*-methyletioporphyrin III in DMF,¹² indicate that activation enthalpies are, at least in part, determined by porphyrin core deformabilities. Based on the present study, we attribute increases in ΔH^{\ddagger} to energetic restrictions on core deformation due to weaker electronic interaction between phenyl rings and the porphyrin macrocycle while increases in ΔS^{\ddagger} (where $\Delta S^{\ddagger}_{\text{total}} = \Delta S^{\ddagger}_{\text{solvated metal ion}} + \Delta S^{\ddagger}_{\text{cplx formation}} + \Delta S^{\ddagger}_{\text{core deformation}}$) could be attributed to changes in $\Delta S^{\ddagger}_{\text{solvated metal ion}}$ for a dissociative mechanism.

Conclusion

Since metal ion incorporation into porphyrins is more complex than simple bimolecular reactions (i.e., Scheme 1), steric effects play a multifaceted role in the metalation process. Steric interactions between ortho substituents and the porphyrin core render the phenyl rings more perpendicular with respect to the porphyrin core as compared to those of non-ortho-substituted TPPs and differentiate the PFPs from meta- and para-substituted TPPs. This "ortho effect" (i.e. effects of ortho substitution on TPP basicities, metalation rate constants, spectral shifts, etc.) is, in part, responsible for the unique physical properties and reactivities of the PFPs although a clear explanation of this effect has been lacking in the literature. Steric interactions between cofacial side chains, resulting in an enhancement of phenyl-to-core perpendicularity (i.e., the transannular effect) over that induced via the ortho effect, are realized as the source of differences in physicochemical properties previously noted for the TPiv atropisomers⁶⁹ and assist interpretation of their metalation rates^{27,32} and ligand binding tendencies.⁷³ On the basis these "transannular" interactions, the phenyl rings of 4,0 PFPs experience restricted mobility about the porphyrin core/phenyl ring single bond resulting in a more rigid porphyrin core. Reduced reactivities noted for the PFPs relative to TPP are attributed to a combination of direct steric exclusion of metal ion by side chains and reduced resonance stabilization via phenyl-to-core conjugation of core-deformed metal ion/porphyrin intermediates (i.e., more rigid cores). Direct steric exclusion of the metal ion is estimated to account for a 7600-fold reduction in metalation rate constant from the hindered face of 4,0 THA relative to TPP while stereoelectronic effects result in up to a 135-fold reduction in core reactivity for 4,0 TPiv relative to TPP.

The relative contributions of direct steric factors, the ortho effect, and transannular steric factors to individual facial metalation rate constants have been calculated. Variations in core deformabilities are attributed to (1) *o*-phenyl substitution/ β -pyrrole steric interactions (the "ortho effect") and (2) transannular steric interactions (particularly steric interactions between adjacent (*cis*) cofacial substituents) based on previous studies (absorption and NMR spectra and atropisomer equilibrium ratios)^{41,65,69} and more conclusive ¹H NMR evidence presented herein and elsewhere.⁶² The UV-visible spectral shifts, ¹H NMR chemical shift patterns in *o*-phenyl resonances of TPP, the 4,0 atropisomers, and molecular models indicate that different degrees of resonance interaction between the phenyl rings and core π systems, which

(106) Reference 8, p 38.

(107) Johnson, N.; Khosropour, R.; Hambright, P. *Inorg. Nucl. Chem. Lett.* **1972**, *8*, 1063.

(108) Hambright, P. J. *Inorg. Nucl. Chem.* **1970**, *32*, 2449.

(109) Adeyemo, A.; Krishnamurthy, M. *Inorg. Chem.* **1977**, *16*, 3355.

(110) See ref 5, p 250.

are subject to phenyl conformation (α), are responsible for variations in core deformabilities for substituted TPPs. Steric exclusion of the metal ion from the porphyrin center, size of the metalating reagent (steric factors), and macrocyclic rigidity induced by alkylamide bulk (stereoelectronic factors) are identified as controlling factors of PFP metalation in homogeneous solution.

Acknowledgment. We are grateful to the National Science

Foundation (Grant CHE-8616361) for funding this work.

Supplementary Material Available: A textual detailed interpretation of the ^1H NMR data and additional discussion, a figure showing limited side chain amide conformations in PFPs, and a listing of shielding factors for side chain resonances of the PFP's (16 pages). Ordering information is given on any current masthead page.

Kinetics of Thermolysis of Ring-Substituted Arylammonium Perchlorates¹

Gurdip Singh* and Inder Pal Singh Kapoor

Department of Chemistry, University of Gorakhpur, Gorakhpur 273009, India (Received: March 27, 1991; In Final Form: August 26, 1991)

Ring-substituted arylammonium perchlorates have been prepared and characterized gravimetrically. Thermal and explosive characteristics of these salts are studied by TG and explosion delay measurements. The explosion temperatures (ET), energies of activation for decomposition (E_d), and explosion (E^*) were found to be linearly related with $\text{p}K_a$ values of the corresponding arylamines. Further, these parameters have also been found to be related with Hammett substituent constant (σ). The proton-transfer process seems to be the primary step involved during decomposition and explosion reactions of these salts.

Introduction

Interest in a systematic study of the characteristics of thermal decomposition of substituted ammonium perchlorates thrives due to the fact that the nitrogen base salts of inorganic acids like HClO_4 and HNO_3 find application in explosive compositions.^{2,3} Because of the presence of both the oxidizer and the fuel groups in the same molecule, they have also been used in propellant formulations.^{2,4} Although the perchlorates of a number of aromatic amines are known,^{5,6} the mechanism of thermal reactions leading to explosions are not yet reported. However, perchlorates are reported⁷ to be more prone to explosion than are the corresponding nitrates. Recently we have reported that the decomposition of dianilinium sulfate,⁸ which is analogous to arylammonium perchlorates, is controlled by random nucleation and the proton-transfer process is the primary step involved during decomposition reactions.

In the present investigation, perchlorates of ring-substituted arylamines have been prepared and characterized. The roles of electron-donating and electron-demanding groups on the thermal stability of these salts have been investigated. The Hammett equation has been found to fit the kinetic data which were estimated from decomposition and explosion delay studies. The proton-transfer process seems to be the rate-controlling step in the decomposition and explosion of ring-substituted arylammonium perchlorates.

Experimental Section

Materials. The following chemicals (obtained from the sources given in parentheses) were purified according to usual methods: aniline (Ranbaxy); *p*-phenylenediamine, *p*-aminobenzoic acid, *o*-toluidine (Thomas Baker, Bombay); *p*-phenitidine, *m*-toluidine, *o*-chloroaniline, *m*-chloroaniline, *p*-chloroaniline, *o*-phenylenediamine (Wilson, Bombay); *m*-nitroaniline (Robert Johnson); *p*-toluidine (BDH); *p*-nitroaniline, *o*-anisidine (CDH, Lucknow).

(1) A part of the work was presented at the National Seminar on Propulsion at Bangalore, India, on Aug 30-31, 1990.

(2) Duglison, C.; Lyerly, W. M.; U.S. Patent 3,431,155, 1969; *Chem. Abstr.* 1969, 70, 116778n.

(3) Lyerly, W. M. U.S. Patent 3,629,021, 1972; *Chem. Abstr.* 1972, 76, 47952.

(4) Lundsgaard, C. J. S. Br. Patent 168,338, 1921; *Chem. Abstr.* 1922, 16, 344.

(5) Spallino, R. *Ann. Chim. Appl.* 1914, 1, 435.

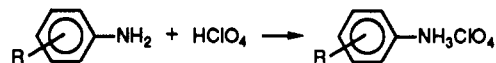
(6) Datta, R. L.; Chatterjee, N. R. *J. Chem. Soc.* 1919, 115, 1006.

(7) Jain, S. R.; Rao, M. V.; Vernecker, P. V. R. *Combust. Flame* 1979, 35, 289.

(8) Singh, G.; Kapoor, I. P. S. *J. Chem. Soc., Perkin Trans. 2* 1989, 2155.

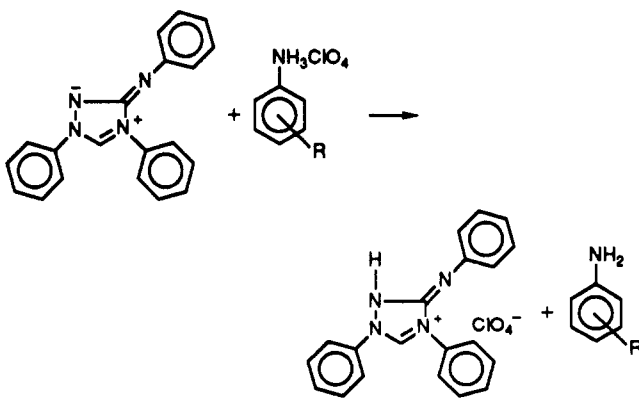
Perchloric acid (60%, Qualigens) was used as received.

Ring-substituted arylammonium perchlorates were prepared by reacting 20% perchloric acid with the corresponding arylamine⁹ in 1:1 molar ratio, and the reaction can be written



where R = H, CH_3 , NH_2 , Cl, NO_2 , OCH_3 , OC_2H_5 , or CO_2H . The monoperchlorates of *o*- and *p*-phenylenediamine were prepared by reacting a calculated amount of amine with HClO_4 acid. All of the perchlorates crystallized out when the volume of the reaction mixture was reduced under reduced pressure at 60 °C by rotary vacuum evaporator (JSGW, Ambala) and then cooled. These were recrystallized from aqueous solution after concentration (under vacuum), and the crystals were vacuum dried; *m*-nitroanilinium, *m*-chloroanilinium, *p*-nitroanilinium and *p*-chloroanilinium perchlorates dissociate in pure water, and hence these were recrystallized from slightly acidic solution.⁵

The purity of these perchlorates was checked by TLC. Further, these were identified by gravimetric method.¹⁰ A slight acidic solution containing a known amount of the perchlorate, heated to incipient boiling, was treated with a solution of nitron reagent¹¹ and the precipitated nitron perchlorate was estimated gravimetrically. The reaction between nitron and amine salt is given by



(9) Schumacher, J. C. *Perchlorates, Their Properties, Manufacture, and Uses*; Reinhold: New York, 1960; p 497.

(10) Arndt, F.; Nachtway. *Ber. Dtsch. Chem. Ges.* 1926, 59B, 446.

(11) Bassett, J.; Denney, R. C.; Jeffery, G. H.; Mendham, J. *Vogel's Text-book of Quantitative Inorganic Analysis*, 4th ed.; Longman: London, 1985; p 497.